AD_____

GRANT NUMBER DAMD17-94-J-4193

TITLE: Protein Kinase C Processes and Their Relation to Apoptosis in Human Breast Carcinoma Cells

PRINCIPAL INVESTIGATOR: John S. Lazo, Ph.D.
Robert L. Rice

CONTRACTING ORGANIZATION: University of Pittsburgh
School of Medicine
Pittsburgh, Pennsylvania 15261

REPORT DATE: August 1997

TYPE OF REPORT: Final

PREPARED FOR: Commander
U.S. Army Medical Research and Materiel Command
Fort Detrick, Frederick, Maryland 21702-5012

REPORT DOCUMENTATION PAGE

Form Approved
OMB No. 0704-0188

1. AGENCY USE ONLY *(Leave blank)*	2. REPORT DATE	3. REPORT TYPE AND DATES COVERED
	August 1997	Final (1 Sep 94 - 31 Aug 97)

4. TITLE AND SUBTITLE
Protein Kinase C Processes and Their Relation to Apoptosis in Human Breast Carcinoma Cells

5. FUNDING NUMBERS
DAMD17-94-J-4193

6. AUTHOR(S)
John S. Lazo, Ph.D.
Robert L. Rice

7. PERFORMING ORGANIZATION NAME(S) AND ADDRESS(ES)
University of Pittsburgh School of Medicine
Pittsburgh, Pennsylvania 15261

8. PERFORMING ORGANIZATION REPORT NUMBER

9. SPONSORING/MONITORING AGENCY NAME(S) AND ADDRESS(ES)
Commander
U.S. Army Medical Research and Materiel Command
Fort Detrick, Frederick, MD 21702-5012

10. SPONSORING/MONITORING AGENCY REPORT NUMBER

11. SUPPLEMENTARY NOTES

12a. DISTRIBUTION / AVAILABILITY STATEMENT
Approved for public release; distribution unlimited

12b. DISTRIBUTION CODE

13. ABSTRACT *(Maximum 200*

Cdc25 phosphatases are possible key oncogenes in human breast carcinoma. In collaboration with Dr. Peter Wipf in the department of Chemistry at the U. of Pittsburgh , it was decided that a promising project would be the development of Cdc25 phosphatase specific inhibitors using combinatorial techniques to test the hypothesis that it is the phosphatase activity that is the main oncogenic function of these oncogenes.

We generated a refined library of novel, phosphate-free, small-molecule compounds synthesized by a parallel, solid-phase combinatorial-based approach. Among the initial 18 members of this targeted diversity library, we identified several inhibitors of DSPases Cdc25A, B and C and the PTPase PTP1B. These compounds at 100 μM did not significantly inhibit the protein serine/threonine phosphatases PP1 and PP2A. Kinetic studies with two members of this library indicated competitive inhibition with K_i values of < 15 μM for Cdc25 DSPases that were also noncompetitive PTP1B inhibitors with K_i values ≤ 1.2 μM. Compound AC-αα69 had a K_i of approximately 10 μM for recombinant human Cdc25A, B and C and a K_i of 0.85 μM for the PTP1B. AC-αaδ9 had antiproliferative activity against and caused a G_1 block in MDA-MB-231 cells.

14. SUBJECT TERMS	15. NUMBER OF PAGES
Apoptosis, Protein Kinase C, Transfection, Activation, Inhibition, Down Regulation, Breast Cancer	58
	16. PRICE CODE

17. SECURITY CLASSIFICATION OF REPORT	18. SECURITY CLASSIFICATION OF THIS PAGE	19. SECURITY CLASSIFICATION OF ABSTRACT	20. LIMITATION OF ABSTRACT
Unclassified	Unclassified	Unclassified	Unlimited

FOREWORD

Opinions, interpretations, conclusions and recommendations are those of the author and are not necessarily endorsed by the U.S. Army.

____ Where copyrighted material is quoted, permission has been obtained to use such material.

____ Where material from documents designated for limited distribution is quoted, permission has been obtained to use the material.

__✓__ Citations of commercial organizations and trade names in this report do not constitute an official Department of Army endorsement or approval of the products or services of these organizations.

____ In conducting research using animals, the investigator(s) adhered to the "Guide for the Care and Use of Laboratory Animals," prepared by the Committee on Care and Use of Laboratory Animals of the Institute of Laboratory Resources, National Research Council (NIH Publication No. 86-23, Revised 1985).

____ For the protection of human subjects, the investigator(s) adhered to policies of applicable Federal Law 45 CFR 46.

__✓__ In conducting research utilizing recombinant DNA technology, the investigator(s) adhered to current guidelines promulgated by the National Institutes of Health.

__✓__ In the conduct of research utilizing recombinant DNA, the investigator(s) adhered to the NIH Guidelines for Research Involving Recombinant DNA Molecules.

__✓__ In the conduct of research involving hazardous organisms, the investigator(s) adhered to the CDC-NIH Guide for Biosafety in Microbiological and Biomedical Laboratories.

PI - Signature

11/28/97

Date

B. Table of Contents

E. Introduction

1. Background

I. Solid Tumors and the cell cycle

Solid tumors such as breast cancer are almost completely refractory to current chemotherapeutic agents, and new drugs that exploit recent biological discoveries are necessary. It is now generally accepted that nearly all forms of neoplasia have altered cell cycle control [5] frequently due to enhanced or altered mitogenic signaling, reduced cell cycle checkpoints, or diminished apoptosis.

Cdc25 phosphatases have been proposed as key oncogenes in human breast carcinoma. In human primary breast cancers tested by Galaktionov et al. overexpression of Cdc25B phosphatase was detected in 32% of patients with axillary node negative invasive breast cancer. Human Cdc25A & B phosphatases also cooperated with Ha-Ras^{G12V} and Cdc25A cooperated with $Rb^{-/-}$ in the oncogenic transformation of mouse embryonic fibroblasts (MEF)[1]. Therefore, phosphorylation signaling pathways involving Cdc25 are potentially rewarding sites in the search for new chemotherapeutic agents and a better understanding of oncogenesis .

II. Cdc25 phosphatases are dual specificity phosphatases

The first dual specificity phosphatase (DSPase) to be discovered, VH1, corresponded to the H1 open reading frame in the vaccinia virus[6]. Several additional members of this family have been discovered such as MAPK phosphatases and, most notably, Cdc25 phosphatases. DSPases can dephosphorylate phosphotyrosine, phosphothreonine, and phosphoserine residues. DSPases in general appear to have a marked preference for protein kinases that are phosphorylated on tyrosine and threonine residues that are in close proximity. This is especially true for certain cyclin dependent kinases. The

substrate motif for Cdc25 phosphatases is -pTpY- [3]. The novel DSPase class, especially Cdc25 phosphatases, are emerging as important regulators of the cell cycle.

III. Cell Cycle and Cdc25 phosphatases

The current model of cell cycle control maintains that the transition between different cell cycle phases are regulated at checkpoints. The integrity of these checkpoints is considered vital in avoiding malignancy. Progression of eukaryotic cells through the cell cycle is controlled in part by the activity of cyclin dependent kinases (cdk) and by protein phosphatases such as Cdc25 phosphatases through a complex phosphorylation cascade[8].

Cdc25 phosphatases are key regulators in the progression of eukaryotic cells from one phase of the cell cycle to the next. The best studied cell cycle event is the transition from G_2 to M phase, in which a nuclear protein complex that contains the catalytic subunit Cdc2 and the regulatory subunit cyclin B has a crucial role. In mammalian cells the activity of Cdc2 is controlled by phosphorylation at three sites [9,10] : T^{161},T^{14}, and Y^{15}. Phosphorylation of T^{161} is absolutely required for activation, while phosphorylation of T^{14} and Y^{15} by wee1 or mik1 inhibits Cdc2 activity. Cdc25C is the most likely human isoform responsible for dephosphorylating Cdc2 at T^{14} and Y^{15} and regulates the G_2/M transition of the cell cycle[9,10]. Other than their oncogenic properties the precise biological functions and role in the cell cycle of the Cdc25A & B phosphatases in the cell cycle are still poorly defined. Cdc25A appears to participate in controlling the cell cycle either at the G_2/M or, more likely, the G_1/S transition where it can be phosphorylated and activated by the cdk2-cyclin E complex [3,4,10]. Cdc25B has recently been proposed to participate in regulating the G_2/M transition [2]. Cdc25 phosphatases in general have an active role in regulating the checkpoints of the cell cycle.

It is known that the phosphatase catalytic domains of Cdc25A and Cdc25B are located within the carboxyl terminus[11]. Although it is generally assumed that the

biological effects of Cdc25 phosphatases are due to intrinsic phosphatase activity, this has been difficult to establish firmly. Attempts to use obvious genetic approaches, such as deletion mutagenesis, have revealed new protein-protein interactions for the mutants with deleted phosphatase activity making conclusions about phosphatase activity and function difficult[11]. Consequently, there is considerable interest in a more pharmacological approach to generate selective antagonists of the phosphatase activity of DSPases. Inhibitors of Cdc25C have potential as selective disrupters of the G_2/M transition, and thus, could be unique antimitotic agents. The Cdc25A and B isoforms could control transition through other domains of the cell cycle and selective antagonists of these DSPases could provide novel cell cycle inhibitors.
These inhibitors also have the potential as apoptotic agents *per se* or enhancers of anticancer drug-induced apoptosis[12].

2. Technical Objectives

(1) Characterize the ability of a small library of novel, nonpeptidic, small-molecules to inhibit Cdc25 phosphatase *in vitro* using recombinant proteins

(2) Examine the selectivity of this inhibition among phosphatases

(3) Determine the antiproliferative activity of these novel compounds with intact cells.

(4) Determine the antiphosphatase activity of these novel compounds with intact cells.

G. Body of Proposal

1. Experimental Methods

Chemical compounds. The generation of the compounds in the combinatorial library has been previously described [16], although we have now adopted a new, more descriptive nomenclature for ease of discussion. The new nomenclature and the compound structures are listed in Figure 1 and Table 1. The basic combinatorial pharmacophore is now termed AC (Figure 1); addition of a phenyl moiety is termed α, a phenethyl is β, benzyl is δ, a styryl is γ and alkyl chains are designated based on the carbon length. Compounds were synthesized using solid bead combinatorial methods and their predicted structural identity and purity (>60%) confirmed by ^{1}H NMR and mass spectroscopy [16]. Several discrete compounds, namely AC-$\alpha\alpha\delta$9 and AC-$\alpha\alpha$69, were synthesized using solution chemistry (SC) according to [16] and are referred to as SC compounds throughout this manuscript to differentiate them from compounds synthesized by solid bead-based combinatorial methods. For the resynthesis of these compounds, 2,2,2-trichlorethoxycarbonyl and allyloxycarbonyl protective groups were used, and amide coupling was effected with BopCl [17] and DPPA [18] coupling agents. We also synthesized for the first time SCα109 and SC-$\alpha\alpha$09 for structural hypothesis testing and used the same procedure as mentioned above for SC-$\alpha\alpha\delta$9 and SC–$\alpha\alpha$69. The SC compounds were >90% pure based on the previously described ^{1}H NMR and mass spectroscopy methods [16]. All compounds were resuspended for biological testing in DMSO as a stock solution of 10 mM and stored in the dark at -70°C in aliquots for use in individual experiments. In contrast to the solid-phase library, which was enriched in the L-stereoisomers, the SC compounds were racemic.

Plasmids and reagents. Plasmid pGEX2T for glutathione-S-transferase (GST)-fusion of full length human Cdc25A was a gift from Dr. Robert T. Abraham

(Mayo Clinic, Rochester, MN) and the plasmids pGEX2T-KG and pGEX2T containing the GST-fusion of full length human Cdc25B and C, respectively, were a gift from Dr. David Beach (Cold Spring Harbor Laboratory, Cold Spring Harbor, NY). The plasmid pET15b containing the histidine-tagged CL100 was a gift from Dr. Stephen M. Keyse (University of Dundee, Dundee, U.K.). The substrate 3,6-fluorescein diphosphate (FDP) was purchased from Molecular Probes Inc. (Eugene, OR), *para*-nitrophenyl phosphate (pNPP) was obtained from Sigma (St. Louis, MO) and Ni-NTA was purchased from Qiagen Inc (Chatsworth, CA). The inhibitory activity of SC-ααδ9 and SC-αα69 against PP1 and PP2A was measured with the phosphatase assay kit from GIBCO-BRL (Grand Island, NY) using PP1 and PP2A catalytic units purified from rabbit skeletal muscle obtained from Upstate Biotechnology (Lake Placid,NY). Phosphorylase b was radiolabeled with Redivue [^{32}P]-γATP, which was from Amersham (Arlington Heights, IL). Alkaline phosphatase from calf intestine was purchased from Promega (Madison, WI). Recombinant PTP1B was obatained from Upstate Biotechnology(Lake Placid, NY).

Bacterial growth and fusion protein production. *E. coli* strain BL21 (DE3) was used for transfection with plasmids containing the fusion constructs encoding GST and Cdc25A, B or C under the transcriptional control of isopropyl β-D-thiogalactopyranoside (IPTG). *E. coli* were first grown overnight at 37°C in the presence of LB media with 100 μg/ml ampicillin. Four ml of this pre-culture was used to inoculate 1 l of LB containing 100 μg/ml of ampicillin. The cultures were incubated at 37°C for 4-5 h. IPTG (1 mM final concentration) was then added and the cultures incubated at 37°C for an additional 3 h. Cells were harvested by centrifugation at 3,500 *g* for 10 min at 4°C. The resultant bacterial pellets were kept frozen at -80°C until extraction. His_6 tagged CL100 was produced similarly except the *E. coli* strain DH5α was used in place of BL21 (DE3).

Purification of GST-fusion proteins. The bacterial pellet was disrupted by sonication at 4°C in lysis buffer containing 10 μg/ml of aprotinin, 10 μg/ml of leupeptin, 100 μg/ml AEBSF and 10 mM DTT. The homogenate was then centrifuged for 10 min at 4°C at 10,000 *g*. The resulting supernatant fraction was immediately mixed and rotated with glutathione beads (equilibrated with lysis buffer) for 1 h at 4°C (5 vol of supernatant / 1 vol of 50% bead slurry). The glutathione beads were washed two times with 10 vol of lysis buffer and then twice with 10 vol of 2x reaction buffer (60 mM Tris , pH 8.5, 150 mM NaCl, 1.34 mM EDTA, 0.066% BSA) containing 10 μg/ml of aprotinin, 10 μg/ml of leupeptin, 100 μg/ml AEBSF and 10 mM DTT. The fusion protein was eluted with 3 successive washes using 10 mM glutathione in 2x reaction buffer. The efficiency of the elution was monitored by the phosphatase assay described below. Active fractions were pooled and supplemented with 20% glycerol prior to storage at -80°C. His_6 tagged CL100 was purified using the same procedure except 20 mM β–mercaptoethanol was used in place of DTT for all steps of the purification and 100 mM imidazole was used instead of 10 mM glutathione for the elution.

Serine/threonine phosphatase assay. The catalytic subunits of PP1 and PP2A were purified from oysters and phosphatase activity was determined with a radiolabeled phosphohistone substrate (histone HI) was determine by the liberation of [^{32}P] using previously described procedures [19, 20]. Briefly, assays were conducted in a final volume of 80 μl containing 50 mM Tris buffer (pH 7.4), 0.5 mM DTT, 1 mM EDTA (assay buffer), phosphohistone (1-2 μM PO_4), and the catalytic subunits of either PP1 or PP2A. Okadaic acid (1 nM) was included in some PP1 preparations to suppress endogenous PP2A activity and had no apparent affect on the inhibitory activity of the compounds tested. Dephosphorylation of [^{32}P]-labeled histone was determined after a 10-20 min incubation with or without 100 μM combinatorial compounds by extraction as a phosphomolybdate complex as described previously [19, 20]. The reaction was directly dependent on enzyme concentration and time under these conditions.

The inhibitory activity of SC-ααδ9 and SC-αα69 against PP1 and PP2A was also measured with rabbit skeletal muscle PP1 and PP2A and [^{32}P] labeled phosphorylase A as a substrate by the commercially available method of GIBCO-BRL.

PTPase and Dual specificity phosphatase assay. The activity of the GST-fusion or His_6 tagged DSPase and PTPase was measured with FDP (Molecular Probes, Inc., Eugene, OR), which is readily metabolized to the fluorescent fluorescein monophosphate [7], as a substrate in a 96-well microtiter plates. The final incubation mixture (150 μl) comprised 30 mM Tris (pH 8.5), 75 mM NaCl, 0.67 mM EDTA, 0.033% bovine serum albumin, 1 mM DTT and 20 μM FDP for Cdc25 phosphatases while the CL100 mixture was at pH 7.0 and the PTP1B mixture was at pH 7.5. Inhibitors were resuspended in DMSO and all reactions including controls were performed at a final concentration of 7% DMSO. Reactions were initiated by adding ~ 0.25 μg of fusion protein and incubated at ambient temperature for 1 h for Cdc25 and Cl100 phosphatase and 30 minutes for PTP1B. Fluorescence emission from the product was measured with a multiwell plate reader (Perseptive Biosystems Cytofluor II; Framingham, MA; excitation filter, 485/20; emission filter, 530/30). For all enzymes the reaction was linear over 2 h of incubation, well within the time used in the experiments, and was directly proportional to both the enzyme and substrate concentration.

Alkaline phosphatase assay. The activity of alkaline phosphatase was measured in a 96-well microtiter plate with FDP (Molecular Probes, Inc., Eugene, OR) as a substrate, which was readily metabolized to the fluorescent fluorescein monophosphate [7]. The final incubation mixture (150 ml) comprised 30 mM Tris (pH 7.3), 75 mM NaCl, 0.67 mM EDTA, 0.033% bovine serum albumin, 1 mM DTT and 1 μM FDP (~ K_m). Inhibitors were resuspended in DMSO and all reactions including controls were performed at a final concentration of 7% DMSO. Reactions were initiated by adding ~ 0.1 unit of alkaline phosphatase and incubated at ambient temperature for 5 min. Fluorescence emission from

the product was measured with a multiwell plate reader (Perseptive Biosystems Cytofluor II; Framingham, MA; excitation filter, 485/20; emission filter, 530/30). For all enzymes the reaction was linear over the time of incubation and directly proportional to both the enzyme and substrate concentration.

Thin-layer chromatography. To ensure that only a single product was produced with the FDP substrate, we incubated FDP and DSPases under our standard reaction condition for 1 h and spotted 2.5 μl of the reaction from each microtiter plate well on a Whatman reversed phase TLC LKC_{18} plate. The resolving conditions were room temperature and a methanol/water (3:2 vol) solvent. Compounds and products were viewed under long UV wavelength (366 nm) to illuminated the potential fluorescein monophosphate and fluorescein product. FDP has no fluorescent intensity at this wavelength. The R_f for fluorescein monophosphate and fluorescein were 0.9 and 0.8, respectively. We found only the fluorescein monophosphate produced under our reaction conditions with the PTPase and DSPases used. Thus, despite the ability of Cdc25 to dephosphorylate fluorescein monophosphate [21], under the reaction conditions used the diphosphate fluorescein was the preferred substrate as previously suggested [12].

Steady-state kinetics. Reactions with GST-Cdc25A, B, and C were conducted in 30 mM Tris (pH 8.5), 75 mM NaCl, 0.67 mM EDTA, 0.033% bovine serum albumin, and 1 mM DTT. Reactions with CL100 were conducted in 30 mM Tris (pH 7.0), 75 mM NaCl, 0.67 mM EDTA, 0.033% BSA, 1 mM DTT, and 20 mM imidazole. Reactions with GST-PTP1B were conducted in 30 mM Tris (pH 7.5), 75 mM NaCl, 0.67 mM EDTA, 0.033% bovine serum albumin, and 1 mM DTT. DMSO was kept at 7% in reaction mixtures to ensure compound solubility. All reactions were carried out at room temperature and product formation determined in an multiwell plate reader (Perseptive Biosystems Cytofluor II; Framingham, MA; excitation filter, 485/20; emission filter, 530/30). Data were collected at 10 min intervals for 1 h for Cdc25 and CL100 phosphatases and 30

minutes for PTP1B. The V_0 was determined for each substrate concentration and then fit to the Michaelis-Menten equation (Equation 1):

$$V_o=V_{max}[S]/(K_m+[S]) \qquad \text{(Eq. 1)}$$

using Prism 2.01 (GraphPad Software Inc.). The correlation coefficient for each experiment and substrate concentration was always >0.9. The substrate concentrations used to determine the steady-state kinetics for Cdc25A, B and C were 10, 20, 30, 40, 50, 75, 100 and 200 μM FDP, for CL100 the concentrations were 75, 100, 200, 300, 400, 500, and 750 μM FDP, and for PTP1B the concentrations were 1, 5, 10, 25, 50, 75, 100, 150 μM FDP.

Determination of inhibition constant. The inhibition constants for SC-ααδ9 and SC- αα69 were determined for the Cdc25 A, B, and C, CL100, and PTP1B hydrolysis of FDP. At various fixed concentrations of inhibitor, the initial rates with different concentrations of FDP were measured. The data were then fit to Equation 2 to obtain the inhibition constant (K_i).

$$V_o=V_{max}[S]/K_m*(1+ [I]/ K_i)+[S]) \qquad \text{(Eq. 2)}$$

$$V_0=V_{max}[S]/((K_m+[S])(1+[I]/K_i)) \qquad \text{(Eq. 3)}$$

At least four concentrations of SC-ααδ9 and SC-αα69 ranging from 0 to 30 μM were used with Cdc25A or B. The K_i of Cdc25C was calculated using at least 4 concentrations of drugs that ranged from 0 to 100 μM of SC-αα69 and SC-ααδ9. At least four concentrations of SC-ααδ9 and SC-αα69 ranging from 0 to 3 μM were used with PTP1B. The K_i of CL100 was determined using 3 different concentrations of SC-ααδ9: 30, 100 and 300 μM.

Cell Culture. Human MDA-MB-231 breast carcinoma cells were obtained from the American Type Culture Collection at passage 28 and were maintained for no longer than 20 passages. The cells were grown in RPMI-1640 supplemented with 1% penicillin (100 μg/mL) and streptomycin (100 μg/mL), 1% L-glutamate, and 10% fetal bovine serum in a humidified incubator at 37^0 C under 5% CO_2 in air. Cells were routinely found free of mycoplasma. To remove cells from the

monolayer for passage or flow cytometry, we washed them two times with phosphate buffer and briefly (< 3 min) treated the cells with 0.05% trypsin/2 mM EDTA at room temperature. After the addition of at least two volumes of growth medium containing 10% fetal bovine serum, the cells were centrifuged at 1,000 x g for 5 min. Compounds were made into stock solutions using DMSO, and stored at -20^{0}C. All compounds and controls were added to make a final concentration of 0.1-0.2% (v/v) of the final solution for experiments.

Cell proliferation assay. The antiproliferative activity of newly synthesized compounds was determined by our previously described method. Briefly, cells (6.5 x 10^3 cells/cm^2) were plated in 96 well flat bottom plates for the cytotoxicity studies and incubated at 37^{0}C for 48 h. The plating medium was aspirated off 96 well plates and 200 μL of growth medium containing drug was added per well. Plates were incubated for 72 h, and then washed 4x with serum free medium. After washing, 50 μL of 3-[4,5-dimethylthiazol-2-yl]-2,5-diphenyl tetrazolium bromide solution (2 mg/mL) was added to each well, followed by 150 μL of complete growth medium. Plates were then incubated an additional 4 h at 37^{0}C. The solution was aspirated off, 200 μL of DMSO added, and the plates shaken for 30 min at room temperature. Absorbance at 540 nm was determined with a Titertek Multiskan Plus plate reader. Biologically active compounds were tested at least 3 independent times.

Measurement of cell cycle kinetics. Cells (6.5 x 10^5/cm^2) were plated and incubated at 37^{0}C for 48 h and then treated with growth medium for 72 h containing a concentration of C3B that caused approximately 50% growth inhibition (88 μM). Untreated cells at a similar cell density were used as control populations. Single cell preparations were fixed in ice-cold 1% paraformaldehyde, centrifugation at 1,000 x g for 5 min, resuspended in Puck's saline, centrifuged, and resuspended in ice-cold 70% ethanol overnight. The cells were removed from fixatives by centrifugation (1,000 x g for 5 min) and stained with a 5 μg/mL propidium iodide and 50 μg/mL RNase A solution. Flow cytometry analyses were conducted with a Becton Dickinson FACS Star. Single parameter DNA histograms were collected for 10,000 cells, and cell cycle

kinetic parameters calculated using DNA cell cycle analysis software version C (Becton Dickinson). Experiments were performed at least 3 independent times.

2. Results

Phosphatase inhibition by solid phase-derived compounds. All members of the current library contained a phenyl substituent on the oxazole C_2 (i.e., R_1) (Table 1). Because the fundamental pharmacophore was based on the PSTPase inhibitors calyculin A, microcystins and okadaic acid, we initially examined the library for its ability to disrupt two established PSTPases. One third of the library members completely failed to inhibit PP1 at 100 μM while more than two thirds of the library inhibited PTP1B with >50% inhibition at 100 μM. Furthermore, at 3 μM several of these compounds still demonstrated >40% inhibition of PTP1B (Table 4).Modest inhibition was observed with the remaining compounds and the maximum reduction in PP1 activity of 32% was seen with AC-ααδβ while this is the one compound that fails to inhibit PTP1B . We found at 100 μM approximately one third of the library members caused >30% inhibition of PP2A with AC-α1δβ, AC-ααδβ and AC-ααδγ causing ~50% inhibition. Although in our preliminary analyses we observed AC-αα19 caused an approximate 50% inhibition of enzyme activity with the PP2A catalytic subunit from bovine cardiac muscle [16], we found no significant inhibition of oyster PP1 or PP2A (Table 2). Okadaic acid (100 μM) and calyculin A (10 nM) were highly effective in our assay and caused >99% inhibition of PP1 or PP2A activity (data not shown). Although no compound at 100 μM produced > 60% inhibition of PP1 or PP2A (Table 2), a preference for compounds with aromatic appointments on R_3 and R_4 with this pharmacophore emerged for these PSTPases. It is interesting that while most of the compounds at 100 μM produced > 50% inhibition of PTP1B(Table 4) only AC-ααδβ, which is one of the most potent PP1 and PP2A inhibitor in the library, failed to inhibit PTP1B.

Several library members also appeared to inhibit DSPases significantly at 100 μM (Table 3). Thus, AC-ααδ9 and AC-αα69 caused >90% inhibition of Cdc25A. AC-α169, AC-α1δ9 and AC-α11γ caused >80% inhibition of Cdc25A, while other compounds, such as AC-αα1β and AC-αα19, had no effect (Table 3). Minor structural modifications of the platform produced marked changes in inhibitory ability consistent with the concept of a restrictive catalytic site in Cdc25 as compared to the PTPase PTP1B.

In general, modification of the R_2 position produced minor changes with no obvious overall preference for phenyl versus methyl among the congeners for Cdc25 phosphatases or PTP1B. The best inhibitors of this series for Cdc25 phosphatases were found when both R_3 and R_4 contained hydrophobic moieties, such as aromatic or extended alkyl species. ACαα69 and ACαα6γ produced a modest (< 30%) inhibition of CL100 activity at 100 μM, but all of the other members of the refined combinatorial library had little or no effect on this MAPK DSPase. Thus, several compounds, such as AC-ααδ9, appeared to have some selectivity for the PTP1B PTPase and Cdc25 DSPases compared to either the MPKP DSPase CL100 or PSTPases.

Concentration dependent inhibition with solid-phase-derived and SC compounds. Analyses of combinatorial library elements required resynthesis of the predicted discrete compound with promising biochemical effects to ensure the inhibitory activity was not associated with a side reactant or contaminants [22]. To investigate more extensively the inhibitory potential of the most active compounds against Cdc25, we next synthesized AC-ααδ9 and AC-αα69 by solution chemistry methods. As illustrated in Figure 2A-D, both solid-phase derived AC-ααδ9 and solution phase derived SC-ααδ9 demonstrated a marked concentration-dependent inhibition of recombinant human Cdc25A and B activity. We observed a half-maximal inhibitory concentration (IC_{50}) of 75 μM for Cdc25A and B when treated with AC-ααδ9, while SC-ααδ9 showed an IC_{50} of

approximately 15 μM for Cdc25A and B (Figure 2A and C). Thus, the SC compounds displayed a 5-fold greater inhibitory activity compared to the solid-phase-derived compounds, which could reflect the increased purity, the inclusion of R-stereoisomers in the racemic SC compounds, or both. Similarly, both AC-ααα69 and SC-ααα69 samples caused a concentration-dependent inhibition of Cdc25A and B with the racemic SC compound being approximately 5-6 fold more potent (Figure 2B and D). The widely used PTPase inhibitor vanadate had an IC_{50} of 1 μM for Cdc25A and B in this assay. To ensure that SC-ααδ9 and SC-ααα69 did not also gained significant activity against PSTPases, we tested these compounds against oyster (data not shown) and rabbit skeletal muscle (Figure 3) PP1 and PP2A catalytic subunit and observed no inhibition at 100 μM. We have seen no inhibition of calf intestine alkaline phosphatase activity with 100 μM of any of the combinatorial library members or with SC ααδ9 or SC-ααα69 (data not shown). Additionally, LeClerc and Meijer (personal communication) also found no inhibition of Cdc2 kinase activity as measure by their previously assay (*23*) with up to 1 mM SCααδ9. Furthermore, okadaic acid, a parent compound on which the pharmacophore platform was based, did not inhibit Cdc25B (Figure 4) demonstrating that the activity was not inherent in the parent compounds. To ensure that the inhibition was not dependent on the FDP substrate, we have also used pNPP as a substrate for Cdc25A and found marked inhibition with SCααδ9, although pNPP was a much poorer substrate than FDP (data not shown). These results confirm and extend studies of Gottlin et al. [21] indicating the aromatic substrate 3-O-methylfluorescein binds with higher affinity and reacts faster with Cdc25B than pNPP. In separate studies, LeClerc and Meijer (personal communication) have observed an IC_{50} of 4 μM with SC-ααδ9 and human recombinant Cdc25A using pNPP and their previously described method [23]. Thus, the results with the solution phase compounds validated the initial observations with the combinatorial library.

Inhibition kinetics of compounds. We next determined the kinetic characteristics of DSPase and PTPase inhibition with SC-ααδ9 and SC-αα69. We found the K_m with FDP for Cdc25A, Cdc25B, Cdc25C, CL100 and PTP1B were 45 ± 3 (SEM, n= at least 4), 12 ±3, 22 ± 1, 192±72 and 21± 9 μM, respectively (Table 5). Therefore, FDP was a much better substrate for Cdc25 and PTP1B phosphatases than for the MAPK phosphatase CL100. Kinetic studies using SC-ααδ9 and SC-αα69 with Cdc25B were most consistent with a competitive inhibition model (Figure 5) while for PTP1B noncompetitive inhibition was the best model (Figure 6). We also concluded SC-ααδ9 competitively inhibits Cdc25A, Cdc25C and CL100 (data not shown) and SC-αα69 competitively inhibits Cdc25A and Cdc25C (data not shown). SC-αα69 had a K_i of 7 ± 3 μM for Cdc25B phosphatase and a K_i of 0.85 ± 06 μM for PTP1B (Table 5). The K_i for Cdc25A and Cdc25C were 8 ± 3 μM and 11 ± 2 μM, respectively (Table 5). The K_i for SC-ααδ9 for the MAPK phosphatase CL100 was 229 ± 115. We have not yet determined the K_i for SC-✂✂69 and CL100.

Based on our initial studies with the library, we predicted that substitution of sterically enriched, hydrophobic moieties on this platform was critical for an efficient inhibitor of Cdc25 and PTP1B. To assess the relative importance of the bulky hydrophobic substitutents on the R_3 position, we synthesized two close congeners of SC-ααδ99 and SC-α1δ9, namely SC-αα09 and SC-α109 (Figure 7A). SC-αα09 had markedly less inhibitory activity at 100 μM compared to SC-α αδ9 and SC-α109 also was less active than SC-α1δ9 (Figure 7B) indicating the importance of the bulky moiety in the R_3 position for Cdc25 phosphatase. SC-αα09 had the same strong inhibitory activity upon PTP1B as SC-ααδ9 demonstrating a bulky moiety at R_3 position was not critical for PTP1B inhibition .

Antiproliferative activity of AC-ααδ9. The effects of AC–ααδ9 in a human breast carcinoma cell line was studied in MDA-MB-231 cells. This cell line was chosen because it expresses Cdc25A & B (data not shown) and has a mutation

in codon 13 giving rise to a Ki-ras^{G14R} mutated allele[15]. This cell line has two of the characteristics necessary for Cdc25 phosphatase related transformation. This makes it an excellent model for testing the effects of inhibiting Cdc25 phosphatase in a cancer cell line.

Only compound AC-ααδ9 demonstrated more than a 50% inhibition of growth among the two (Figure8.). Therefore, we first evaluated the antiproliferative activity of combinatorial AC-ααδ9 in MDA-MB-231 cell lines in a concentration-response study using our previously described MTT microtiter assay [16,17]. We also characterized the cell cycle phase-specificity of the inhibitor AC-ααδ9. Asynchronous growing MDA-MB-231 cells were treated with SC-ααδ9 to investigate gross cell cycle perturbations using flow cytometry. The biological effect of AC-ααδ9 in these include: antiproliferative activity with an IC_{50} ~ 100 μM in MDA-MB-231 cells and a definite G_1 block upon treatment with 88 μM. (Figure 9)

H. Conclusions

It was reported previously that the specific aim of screening agents that would induce apoptosis in the human breast carcinoma cell line MDA-MB-231 was completed, and that calyculin A was the most effective compound tested. Since then Cdc25 phosphatases were reported as possible key oncogenes in human breast carcinoma[1]. In light of our results with calyculin A and an ongoing collaboration with Dr. Peter in evaluating a combinatorial library of calyculin A analogues, it was decided that a more opportune focus for the project would be the biochemical basis for the oncogenic actions of Cdc25 phosphatases in human breast carcinoma.

Combinatorial chemistry provides a powerful new approach to diversify the structure of biologically active natural products [22]. In this study we have developed a refined chemical scaffold for targeted combinatorial chemistry based on a predicted pharmacophore obtained from the structure activity

relationship of several natural product inhibitors of PSTPases. Although the side chain composition and the size of the initial library is rather limited at this time, the pharmacophore was readily functionalized and proved to be a most promising platform for future compound syntheses. It is noteworthy that none of the compounds in the library had highly efficacious inhibitory activity against PSTPases despite the use of a pharmacophore that owed its original design to natural product PSTPase inhibitors.

A detailed analysis of the structure-activity profile is limited by the relatively small library size, however certain observations can be made concerning the inhibition of PSTPase, Cdc25 phosphatase and the PTPase PTP1B. Clearly the ability of some of the library compounds, such as AC-$\alpha\alpha\delta\beta$, to modestly inhibit both PP2A and Cdc25 phosphatases while having little effect on PTP1B indicates an overlapping inhibitor specificity between the PSTPases and Cdc25 enzyme. Nonetheless, distinct specificities emerged between PP2A phosphotase and the Cdc25 and PTP1B phosphatases. The nonyl moiety has greater steric bulk and is more hydrophobic (logP > 4) compared to either the phenethyl (logP=3.15) or styryl (logP=2.95) moieties. Substitution of the nonyl moiety at the R_4 site of a compound containing a phenyl at R_2 and a benzyl at R_3 (Figure 1) caused a significant increase in Cdc25 phosphatase inhibition and a complete loss of PSTPase inhibition as compared to the substitution of the phenethyl or styryl moiety at R_4. This may reflect a hydrophobic region on Cdc25 near the active site. Interestingly, Sodeoka et al. [11] found the hydrophobic side chain of RK-682 was important for the inhibitory activity against Cdc25 but not VHR In contrast to Cdc25 phosphatases, the PSTPases were much less tolerant of bulky, hydrophobic substitutions at R_4 and none of the R_4 nonyl compounds were effective inhibitors of PP1 or PP2A while AC-α169 and AC-$\alpha 1\delta$ 9 were respectable inhibitors of Cdc25A and B and PTP1B phosphatase(Table 3 and 4).

The identification of inhibitors of PTPases and DSPases most likely reflects the lack of sequence similarity between the PSTPase, PTPase and DSPases and the distinct fundamental catalytic mechanisms that exist between PSTpases and the enzyme superfamily of PTPases and DSPases [1, 21, 23]. The crystal structure of the catalytic sites of prototype PSTPase , PTPases and DSPases also suggest they would accommodate different substrates and inhibitors consistent with previous biochemical studies [19]. Consequently, the identification of inhibitors that exhibit selectivity to the Cdc25 class of DSPase and the PTPase PTP1B is consistent with our current understanding of these phosphatases. The Cdc25 class of DSPases share <10% amino acid identity with the MAPK phosphatase class of DSPase and PTPase PTP1B and no common intervening amino acids in the critical HCXXXXXR active. Consequently, a preference of several members of the library for the PTP1B PTPase and Cdc25 class of phosphatases over the MAPK phosphatase class can be rationalized. Because the catalytic region of the Cdc25 enzymes, namely HCEFSSER, are identical, the similar K_i values for Cdc25A, B or C with SC-ααδ9 or SC-αα69 are not surprising.

In summary, we have identified a new class of small molecule, competitive, inhibitors of human Cdc25 DSPases and noncompetitive inhibitors of PTP1B PTPase that are readily synthesized. Moreover, there is some evidence that PP2A and Cdc25 phosphatases have overlapping yet distinct inhibitor specificity. These compounds are small and lack phosphates, which should increase their ability to enter cells. We previously demonstrated [16] that AC-ααδ9 caused a concentration-dependent inhibition of human breast cancer MDA-MB-21 cell proliferation and a G_1 cell cycle block consistent with intracellular entry. We are currently attempting to determine if these cellular effects are mediated by phosphatase inhibition. The pharmacophore used in our present studies should provide an excellent platform for future analog development. Our results illustrate the potential usefulness of this combinatorial-based approach in generating lead structures for selective inhibitors for phosphatases.

We have accomplished the first and second objective of this project by demonstrating the ability of a small library of novel, nonpeptidic, small-molecules to inhibit Cdc25 phosphatase selectively *in vitro* using recombinant proteins. We have also accomplished the third objective by determining the antiproliferative and cell cycle effects of the compound SC-$\alpha\alpha\delta$9. The fourth objective, to determine the antiphosphatase activity of these novel compounds with intact cells, has just been initiated , and as of yet there is no data to report.

I. Bibliography

1. Galaktionov,K., Lee,A., Eckstein,J., Draetta,G., Mekler,J., Loda,M., and Beach, D. CDC25 Phosphatases as Potential human Oncogenes Science 269,1575-1577,1995.
2. Gabriell, B.G.,De Souza, C., Tonks, I., Clark,J., Hayward, N., and Ellem,K. Cytoplasmic Accumulation of CDC25B Phosphatase in Mitosis Triggers centrosomal microtubule nucleation in Hela cells. J. Cell. Sci. 109,1081-1093,1996.
3. Jinno, S., Suto, K. Nagata, A., Igarashi, M., Kanaska, V., Nojma, H., and Okayama, H. CDC25 is a Novel Phosphatase Functioning early in the Cell Cycle. EMBO J. 13,1549-1556,1994.
4. Gautier, J., Solomon, M., Booha, R., Bazan, F., and Kirschner, M. CDC25 is a specific Tyrosine Phosphatase that Directly Activates $p34^{CDC2}$. Cell 67, 197-211, 1991.
5. Hoffmann, I., Draetta, G., Karsenti,E. Activation of the Phosphatase Activity of Human CDC25A by a CDK2-Cyclin E Dependent Phosphorylation at the G_1/S Transition. Embo J. 13,4302-4310, 1994.
6. Guan, K., Hakes, D.J., Wang, Y., Park, H., Cooper, T., and Dixon, J.E. A Yeast Protein Phosphatase Related to the Vaccinia Virus VH1 Phosphatase Induced by Nitrogen Starvation. Proc. Natl. Acad. Sci. 89, 12170-12175,1992.
7. Sherr, C. G_1 Phase Progression: Cycling on Cue. Cell 79,551-555, 1994.
8. Norbury, C and Nurse P. Animal Cell Cycle and Their Control. Ann. Rev. Biochem. 61: 441-470, 1992.
9. Hunter, T. and Pines, J. Cyclins and Cancer II: Cyclin Dependent Kinases and CDK Inhibitors Come of Age. Cell 79: 573-582,1994.
10. Terade, V., Tatsuka, S., Jinne, S., and Okayama, H. Requirement for Tyrosine Phosphorylation of CDK4 in G_1 Arrest Induced by Ultraviolet Irradiation. Nature 376:358-362,1995.

11. Xu, X. and Burke, S.P. Roles of active site residues and the NH2-terminal domain in catalysis and substrate binding of human cdc25. J. Biol. Chem. **271**: 5118-5124, 1996.

12. Ongkeko, W., Ferguson, D.J.P., Harris, A.L. and Norbury, C. Inactivation of Cdc2 increases the level of apoptosis induced by DNA damage. J. Cell Sci. **108**: 2897-2904, 1995.

13. Schmidt, A., Rutledge,S., Endo, N., Opas, E., Tanaka, H., Wesolowski, G., Huang, Z., Ramachandaran, C., Rodan,S., and Rodan, G. Protein Tyrosine Phosphatase Activity Regulates Osteoclast Formation and Function: Inhibition by Alendronate. Proc. Natl, Acad. Sci. 93, 3068-3073, 1996.

14. Denu, J., Zhou, G. Wu, L. Zhao, R., Yovaniyama, J., Saper, M., Dixon, J.E. The Purification and Characterization of a Human Dual Specific Protein Tyrosine Phosphatase. J. Biol. Chem. 270, 3796-3803, 1995.

15. Kozma, S., Bogaard, M., Buser, K., Sauer, S., Bos, J., Bernd, G., and Hynes, N. the Human c-Kirsten Ras Gene is Activated by a Novel Mutation in Codon 13 in the Carcinoma Cell Line MDA-MB-231. Nucleic Acids Research 15, 5963-5971, 1987.

16. Wipf, P., Cunningham, A., Rice, R. L., and Lazo, J. S. (1997) *Bioorg. Med. Chem. 5*, 165-178

17. Coste, J., Frerot, E., and Jouin, P. (1994) *J. Org. Chem. 59*, 2437-2446

18. Shioiri, T., Ninomiya, K., and Yamada, S. (1972) *J. Amer. Chem. Soc. 94*, 6203-6205

19. Honkanen, R. E., Codispoti, B., Tse, K., and Boynton, A. L. (1994) *Toxicon 32*, 339-350

20. Honkanen, R. E., Dukelow, M., Zwiller, J., Moore, R. E., Khatra, B. S., and Boynton, A. L. (1991) *Molec. Pharmacol. 40*, 577-583

21. Gottlin, E. B., Xu, X., Epstein, D. M., Burke, S. P., Eckstein, J. W., Ballou, D. P., and Dixon, J. E. (1996) *J. Biol. Chem. 271*, 27445-27449

22. Ellman, J., Stoddard, B. and Wells, J. Combinatorial thinking in chemistry and biology. Proc. Natl. Acad. Sci. USA. *94*, 2779-2782, 1997.

23. Baratte, B., Meijer, L., Galaktionov, K., and Beach, D. (1992) *Anticancer Res. 12*, 873-880

24. Yuvaniyama, J., Denu, J. M., Dixon, J. E., and Saper, M. A. (1996) *Science 272*, 1328-133

25. Hoffmann, I., Draetta, G., and Karsenti, E. (1994) *EMBO J. 13*, 4302-4310

26. Jinno, S., Suto, K., Nagata, A., Igarashi, M., Kanaoka, Y., Nojima, H., and Okayama, H. (1994) *EMBO J. 13*, 1549-1556

27. Galaktionov, K., Lee, A. K., Eckstein, J., Draetta, G., Meckler, J., Loda, M., and Beach, D. (1995) *Science 269*, 1575-1577

28. Galaktionov, K., Chen, X., and Beach, D. (1996) *Nature 382*, 511-517

J. Addendum

1. Statement of Work

Function of Cdc25 Phosphatase in the Development of Human Breast Cancer

Task I. Characterize the ability of a small library of novel, nonpeptidic, small-molecules to inhibit Cdc25 phosphatase *in vitro* using recombinant proteins. Months 1-15

1. Evaluation for DSPase activity
   - **a)** Microtiter assay for dephosphorylation to evaluate intial library elements using recombinant Cdc25A,B, C currently being made in our laboratory.
   - **b)** Complete kinetic analysis will be done on all highly active compounds

Task II. Examine the selectivity of this inhibition among phosphatases. Months 15-24

1. Primary evaluation for DSPase activity
   - **a)** Microtiter assay for dephosphorylation to evaluate intial library elements using recombinant Cdc25A,B, &C and CL100 currently being made in our laboratory and VHR, PTP1B, PP1, PP2A and PP3.
   - **b)** Complete kinetic analysis will be done on all highly active compounds.
2. Secondary evaluation for DSPase activity
   - **a)** Primary assay permits rapid analysis, but the artificial substrate used may not fully emulate enzyme-substrate interactions. Therefore, once we have identified an active compound, we will use phosphopeptide substrates to determine all four possible phosphorylation states of the peptide in the presence and absence of the active compound by HPLC assay.

Task III. Determine the antiproliferative activity of these novel compounds with intact cells. Months 22-36.

1. We will use the previously described MTT microtiter assay to determine the antiproliferative and cytotoxicity activity of this initial combinatorial library using MDA-MB-231 cells .
   - **a)** Concentration-response curve

b) Time studies

Task IV. Determine the antiphosphatase activity of these novel compounds with intact cells.

1) I.P kinase activity of cdk complexes to determine effects of AC-ααδ9 on MDA-MB-231 cells
- **a)** CDK complexes
  - **I.** Cdc2 complexes
  - **II.** Cdk2 complexes
  - **III.** Cdk4/cdk6 complexes
- **b)** Time course study
- **c)** Concentration response study

2) Western blot to detect tyrosine phosphorylation status of relevant CDK complexes if **Task III. 1)** shows inhibition of CDK complexes to rule out non-specific or indirect effects by AC-ααδ9.

3) Western blot to detect any possible CDKI induction if **Task III. 1)** shows inhibition of CDK complexes to rule out non-specific or indirect effects by AC-ααδ9.

4) I.P. kinase activity of MAPK & SAPK to rule out non-specific or indirect effects of dual-specificity inhibition by AC-ααδ9
- **a)** Time course study
- **b)** Concentration response study

2. Training

In fulfillment of my doctoral training, I have completed all required course work and comprehensive exam, and I am currently a Ph.D. candidate. I have had my first thesis committee this July 8, 1996, and plan to have my second meeting this mid-October, 1996 to finalize my thesis goals with my committee. I participate in the Predoctoral training Program in Breast Cancer Biology and Therapy, and regularly attend seminars.

3. Figures

Figure 1. General chemical structure of pharmacophore.

Figure 2. Concentration-dependent inhibition of Cdc25A and B phosphatase by AC-ααδ9, SC-ααδ9, AC-αα69 and SC-αα69. Compounds AC-ααδ9 and AC-αα69 are indicated by open symbols and compounds SC-ααδ9 and SC-αα69 by closed symbols. Panel A. Inhibition of recombinant human Cdc25A phosphatase activity by SC-ααδ9 and AC-ααδ9; Panel B. Inhibition of recombinant human Cdc25A phosphatase activity by SC-αα69 and AC-αα69; Panel C. Inhibition of recombinant human Cdc25B phosphatase activity by SC-ααδ9 and AC-ααδ9; Panel D. Inhibition of recombinant human Cdc25B phosphatase activity by SC-αα69 and AC-αα69; N=3; Bar=SEM. Enzymatic activities were determined as outlined in Material and Methods Section and fit by the curve fitting program in Prism 2.01.

Figure 3. Inhibition of PP1 and PP2A by 100 μM SC-ααδ9 and SC-αα69. Controls are open bars and cross-hatched bars represent 10 nM calyculin A treatment while compounds SC-αα69 and SC-ααδ9 are indicated by horizontal and filled striped bars, respectively; N=3; Bar=SEM. Enzymatic activities were determined as outlined in the Material and Methods Section with rabbit skeletal muscle catalytic subunits.

Figure 4. Effect of okadaic acid and SC-ααδ9 on Cdc25B phosphatase activity. Various concentrations of okadaic acid -(▲)- and SC-ααδ9 -(■)- were incubated with recombinant human Cdc25B as described in the Material and Methods Section. The resulting data were fitted to the curve Prism 2.01. N=3; Bar=SEM.

Figure 5. Kinetic analyzes of Cdc25B inhibition by SC-ααδ9 and SC-αα69. In panel A and B -■- represented 0 μM inhibitor concentration, -▲- was 10 μM, -▼- was 15 μM and -◆- was 30 μM. In panel C and D -■- represented 0 μM, -▲- was 3 μM, -▼- was 10 μM, -◆- was 15 μM and -●- was 30 μM . Panel A. Michaelis-Menten plot of Cdc25B inhibition by SC-ααδ9. ; Panel B. Hanes - Woolf plot of Cdc25B inhibition by SC-ααδ9; Panel C. Michaelis-Menten plot of Cdc25B inhibition by SC-αα69. ; Panel D. Hanes -Woolf plot of Cdc25B inhibition by SC-αα69; N=5. Enzyme activities were determined as outlined in Material and Methods Section and the data fit to the non-linear Michaelis-Menten equation while all the data points were also fit simultaneously to the Hanes-Woolf equation for competitive inhibition for the Hanes-Woolf plot by the curve fitting program Prism 2.01. The values reported under "Results" for Km and Ki were calculated from a nonlinear fit of the data to the Michaelis-Menten equation for competitive inhibition using the same program.

Figure 6. Kinetic analyzes of PTP1B inhibition by SC-ααδ9 and SC-αα69.

-■- represented 0 μM inhibitor concentration, -▼- was 0.1 μM, -◆- was 0.3 μM, -●- was 1 μM, and -□- was 3 μM. Panel A. Michaelis-Menten plot ofPTP1B inhibition by SC-ααδ9. ; Panel B. Hanes -Woolf plot of PTP1B inhibition by SC-ααδ9; Panel C. Michaelis-Menten plot of PTP1B inhibition by SC-αα69. ; Panel D. Hanes -Woolf plot of PTP1B inhibition by SC-αα69; N=4. Enzyme activities were determined as outlined in Material and Methods Section and the data fit to the non-linear Michaelis-Menten equation while all the data points were also fit simultaneously to the Hanes-Woolf equation for competitive inhibition for the Hanes-Woolf plot by the curve fitting program Prism 2.01. The values reported under "Results" for Km and Ki were calculated from a nonlinear fit of the data to the Michaelis-Menten equation for noncompetitive inhibition using the same program.

Figure 7. Chemical structure and inhibition of SC-αα09 and SC-α109. Panel A. Chemical structures of SC-αα09 and SC-α109. Panel B. Inhibition of Cdc25C phosphatase activity as described by the procedures in the Materials and Methods Section. All values are expressed as a percent of vehicle control and the compound concentration was 100 μM. N=3; Bars=SEM. Panel C. Inhibition of PTP1B phosphatase activity as described by the procedures in the Materials and Methods Section. All values are expressed as a percent of vehicle control and the compound concentration was 100 μM. N=3; Bars=SEM.

Figure 8. Antiproliferative effect of compound AC-ααδ9 against human MDA-MB-231 breast cancer cells.

Figure 9. Cell cycle distribution of human breast cancer cells after treatment with compound AC-ααδ9 determined by flow cytometry. Panel A. Flow cytometry analysis of MDA-MB-231 cells treated with vehicle alone. Panel B. Flow cytometry analysis 48h after treatment with 88 μM compound AC-ααδ9. Fluorescence channel measures intracellular propidium iodide concentration, and index of DNA content. Horizontal bars are the gating positions that allow for cell cycle analysis. Panel C. MDA-MB-231 cell cycle distribution 48h after continuos treatment with 88 μM compound AC-ααδ9. This is the result of one experiment. Open bars are control cells and black bars are cells treated with compound Ac-aad9. Panel D. Cell cycle distribution 72h after continuous treatment with 88 μM AC-ααδ9. The mean values were obtained from three independent determinations. Open bars are control and black bars are cells treated with 88 μM. AC-ααδ9. The SE of the mean are displayed.

Table 1

Compound	R_1	R_2	R_3	R_4
AC-α119		CH_3	CH_3	$n\text{-}C_9H_{19}$
AC-α169		CH_3	$n\text{-}C_6H_{13}$	$n\text{-}C_9H_{19}$
AC-α1δ9		CH_3		$n\text{-}C_9H_{19}$
AC-αα19			CH_3	$n\text{-}C_9H_{19}$
AC-αα69			$n\text{-}C_6H_{13}$	$n\text{-}C_9H_{19}$
AC-ααδ9				$n\text{-}C_9H_{19}$
AC-α11β		CH_3	CH_3	
AC-α16β		CH_3	$n\text{-}C_6H_{13}$	
AC-α1δβ		CH_3		
AC-αα1β			CH_3	
AC-αα6β			$n\text{-}C_6H_{13}$	
AC-ααδβ				
AC-α11γ		CH_3	CH_3	
AC-α16γ		CH_3	$n\text{-}C_6H_{13}$	
AC-α1δγ		CH_3		
AC-αα1γ			CH_3	
AC-αα6γ			$n\text{-}C_6H_{13}$	
AC-ααδγ				

TABLE 2. *Inhibition of PSTPase activity with 100 μM combinatorial compound.*

Compound	PP1		PP2A	
	% Inhibition			
	Mean	SEM	Mean	SEM
AC-α119	0	0	0	0
AC-α169	4	10	14	15
AC-α1δ9	11	3	33	13
AC-αα19	0	0	0	0
AC-ααδ9	0	0	0	0
AC-ααδ9	9	7	5	11
AC-α11β	12	6	15	11
AC-α16β	11	5	31	10
AC-α1δβ	13	1	48	8
AC-αα1β	22	2	20	4
AC-αα6β	1	19	32	21
AC-ααδβ	32	5	47	6
AC-α11γ	11	4	13	4
AC-α16γ	27	9	23	2
AC-α1δγ	25	3	35	4
AC-αα1γ	27	5	8	11
AC-αα6γ	17	9	40	9
AC-ααδγ	24	9	46	8

Each value is the % inhibition from untreated control and the mean from three independent determinations.

TABLE 3. *Inhibition of DSPase activity with 100 μM combinatorial compound.*

Compound	Cdc25												MAPKP			
	Cdc25 A		Cdc25 A		Cdc25 B		Cdc25 B		Cdc25 C		Cdc25 C		CL100		CL100	
	% Inhibition															
	Exp. 1		Exp. 2		Exp. 1		Exp. 2		Exp. 1		Exp. 2		Exp. 1		Exp. 2	
	Mean	SEM	Mean	SEM	Mean	SEM	Mean	SEM	Mean	SEM	Mean	SEM	Mean	SEM	Mean	SEM
AC-α119	35	3	30	1	0	0	0	0	6	3	0	0	10	3	5	6
AC-α169	86	2	86	2	53	1	60	1	11	1	28	1	16	4	21	5
AC-α189	90	1	88	3	55	1	60	2	44	2	35	5	19	3	0	0
AC-αα19	0	0	3	2	9	2	8	1	33	2	21	2	0	0	18	6
AC-αα69	95	4	92	3	82	1	84	2	64	3	56	1	26	4	27	6
AC-αα89	97	2	97	1	84	1	87	5	56	3	60	2	0	0	12	10
AC-α11β	48	3	52	5	42	10	0	0	18	1	2	1	0	0	0	0
AC-α16β	70	2	58	4	44	4	18	3	17	2	14	2	0	0	0	0
AC-α18β	77	2	62	2	35	1	38	1	21	8	28	2	0	0	0	0
AC-αα1β	0	0	0	0	9	1	11	6	46	2	31	1	0	0	0	0
AC-αα6β	20	4	15	2	24	1	24	2	27	4	40	4	0	0	4	6
AC-αα8β	48	1	29	1	30	2	32	3	57	5	51	2	0	0	0	0
AC-α11γ	85	4	77	1	53	1	57	1	54	1	52	2	0	0	0	0
AC-α16γ	78	5	64	1	34	1	34	3	30	2	33	1	0	0	0	0
AC-α18γ	76	3	55	1	34	1	34	3	37	4	36	1	0	0	0	0
AC-αα1γ	31	3	27	4	7	5	20	3	48	2	51	2	0	0	4	6
AC-αα6γ	48	2	43	2	46	3	29	2	52	6	51	1	25	5	21	1
AC-αα8γ	73	2	43	3	57	3	31	6	66	3	56	3	0	0	0	0

Each value is the % inhibition from untreated control and the mean from an experiment done in triplicate.

TABLE 4. *Inhibition of PTPase activity with combinatorial compound.*

Compound	3 μM		100 μM	
	% Inhibition			
	Mean	SEM	Mean	SEM
AC-α119	0	0	32	7
AC-α169	15	6	77	7
AC-α1δ9	48	3	85	9
AC-αα19	3	7	38	10
AC-αα69	37	9	91	13
AC-ααδ9	40	2	92	3
AC-α11β	43	12	91	5
AC-α16β	50	7	61	14
AC-α1δβ	5	7	59	7
AC-αα1β	41	26	50	8
AC-αα6β	35	24	63	13
AC-ααδβ	3	10	1	16
AC-α11γ	0	0	45	3
AC-α16γ	38	3	74	8
AC-α1δγ	5	7	80	9
AC-αα1γ	41	26	52	7
AC-αα6γ	42	7	48	13
AC-ααδγ	42	7	79	12

Each value is the % inhibition from untreated control and the mean from at least three independent determinations.

Table 5. K_m and inhibition constant of SC-ααδ9 and SC-αα69 for DSPases and PTPases.

Compound*	K_m (μM)		K_i for SC-ααδ9 (μM)		K_i for SC-αα69 (μM)	
	Average	SEM	Average	SEM	Average	SEM
Cdc25A	45	3	9	2	8	3
Cdc25B	12	3	6	2	7	3
Cdc25C	22	1	11	3	11	2
CL100	192	72	229	115	ND	ND
PTP1B	21	9	1.2	0.2	0.85	0.06

ND = Not determined

* n = 3-10 independent experiments

Figure 1

AC - R_1 R_2 R_3 R_4

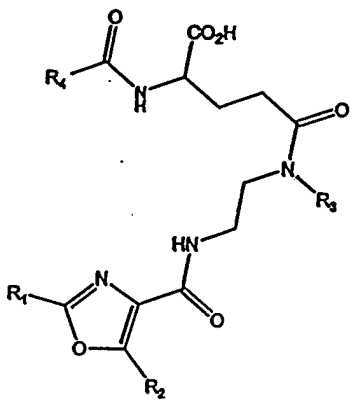

Figure 2

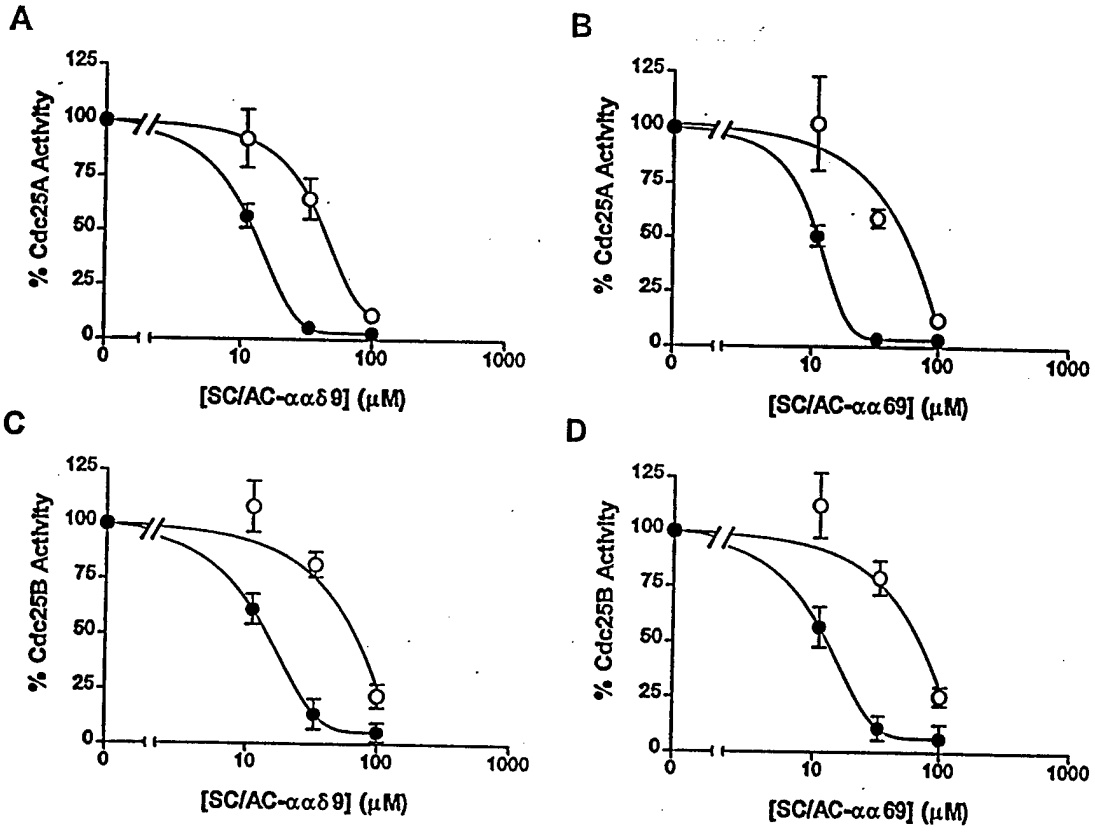
A
% Cdc25A Activity
125
100
75
50
25
0
0
10
100
1000
[SC/AC-αaδ9] (μM)
B
% Cdc25A Activity
[SC/AC-αa69] (μM)
C
% Cdc25B Activity
[SC/AC-αaδ9] (μM)
D
% Cdc25B Activity
[SC/AC-αa69] (μM)

Figure 3

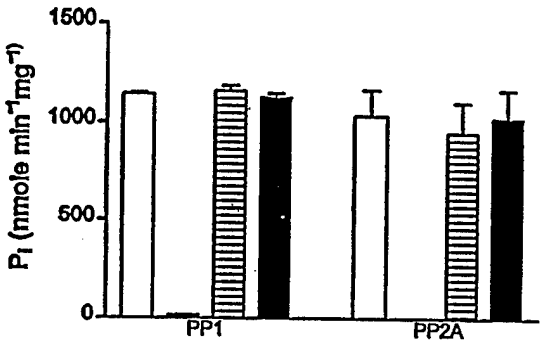

Figure 4

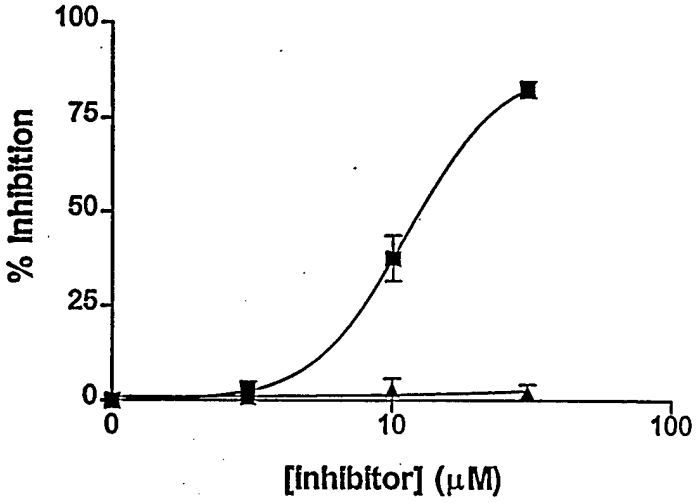

Figure 5

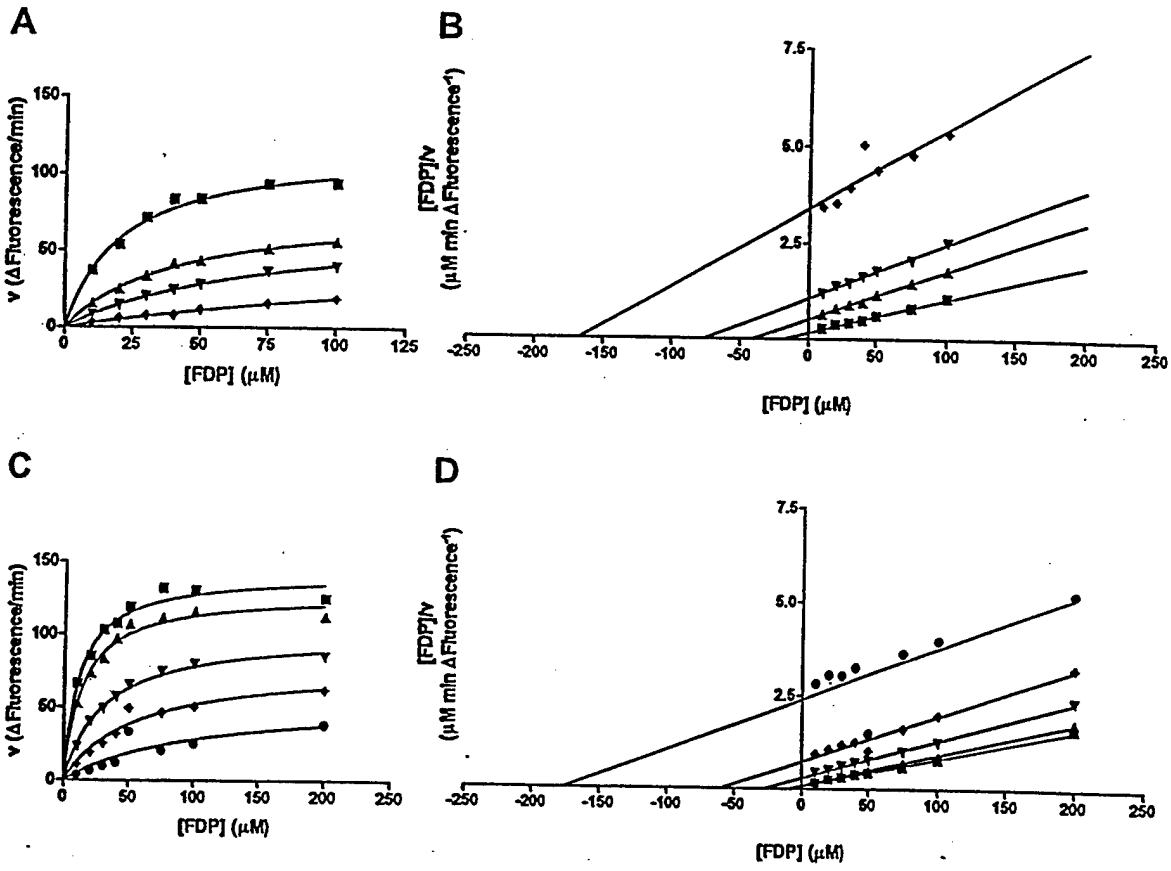
A
v (ΔFluorescence/min)
[FDP] (μM)
B
[FDP]/v
(μM min ΔFluorescence⁻¹)
[FDP] (μM)
C
v (ΔFluorescence/min)
[FDP] (μM)
D
[FDP]/v
(μM min ΔFluorescence⁻¹)
[FDP] (μM)

Figure 6

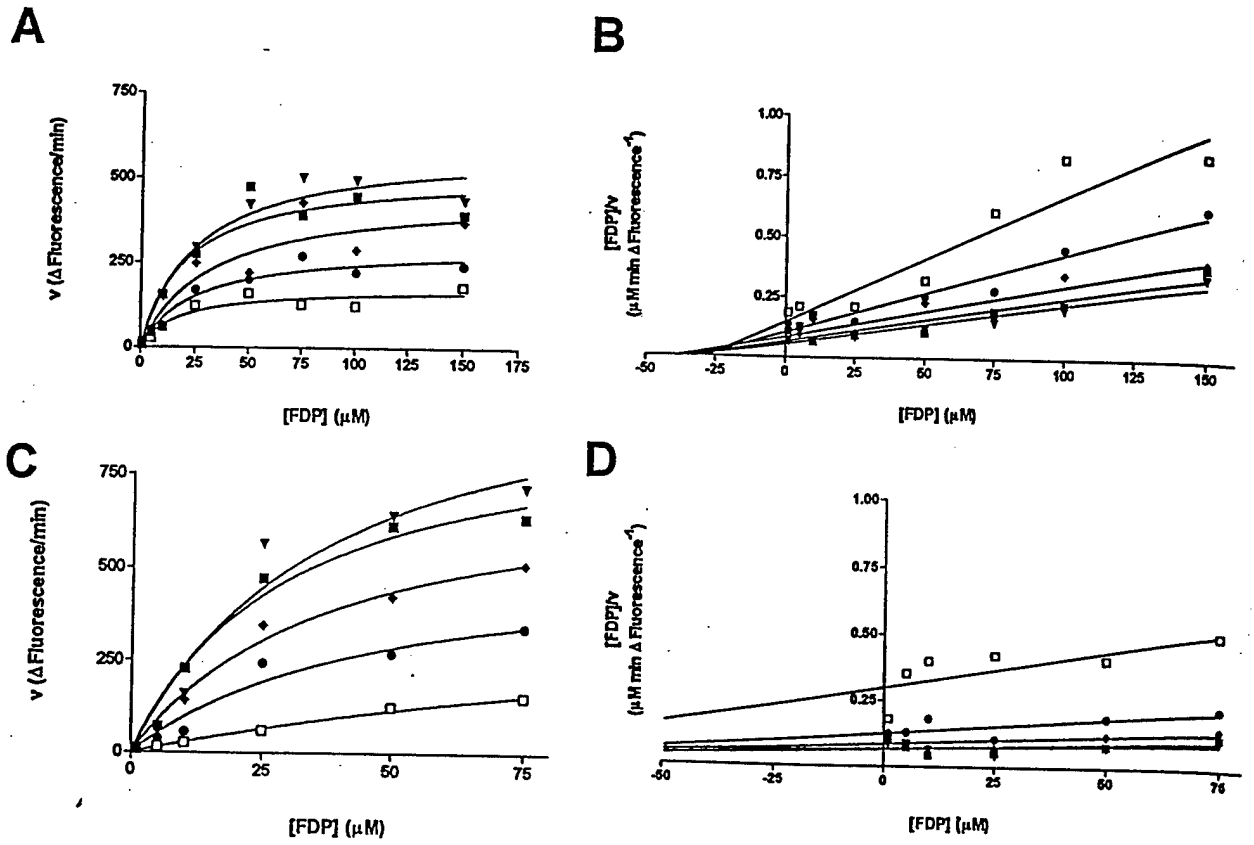
A
v (Δ Fluorescence/min)
750
500
250
0
0
25
50
75
100
125
150
175
[FDP] (μM)
B
[FDP]/v
(μM min Δ Fluorescence⁻¹)
1.00
0.75
0.50
0.25
-50
-25
0
25
50
75
100
125
150
[FDP] (μM)
C
v (Δ Fluorescence/min)
750
500
250
0
0
25
50
75
[FDP] (μM)
D
[FDP]/v
(μM min Δ Fluorescence⁻¹)
1.00
0.75
0.50
0.25
-50
-25
0
25
50
75
[FDP] (μM)

A

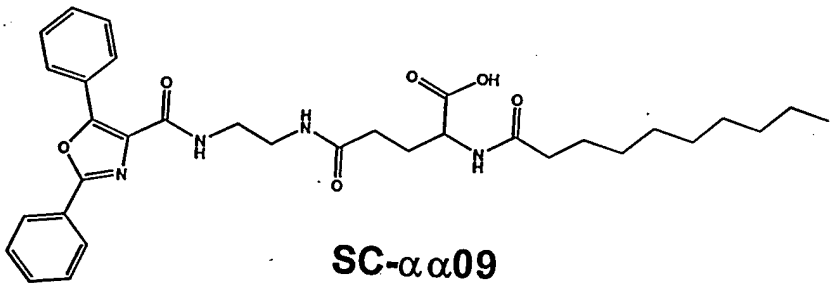

SC-αα09

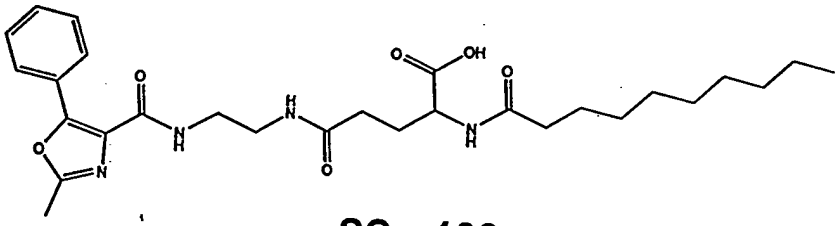

SC-α109

B

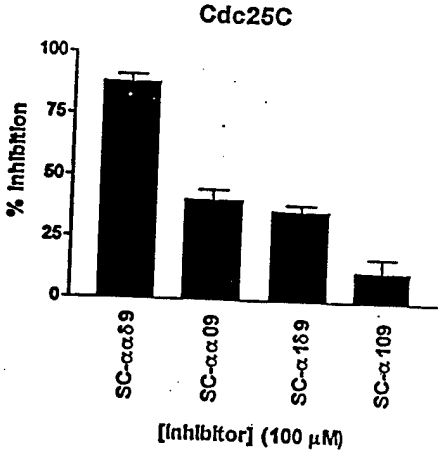

C

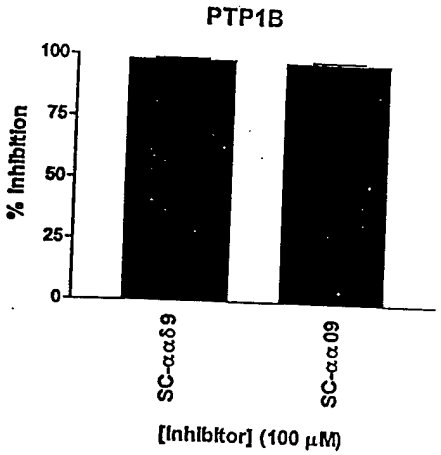

Figure 8

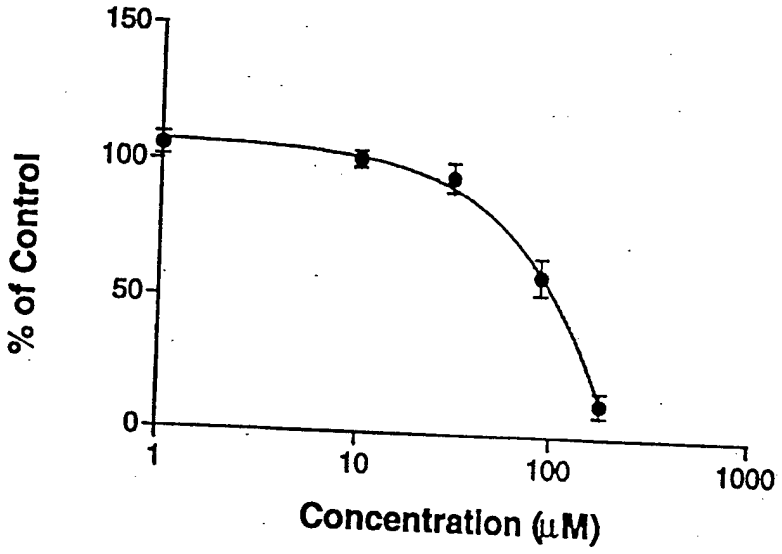

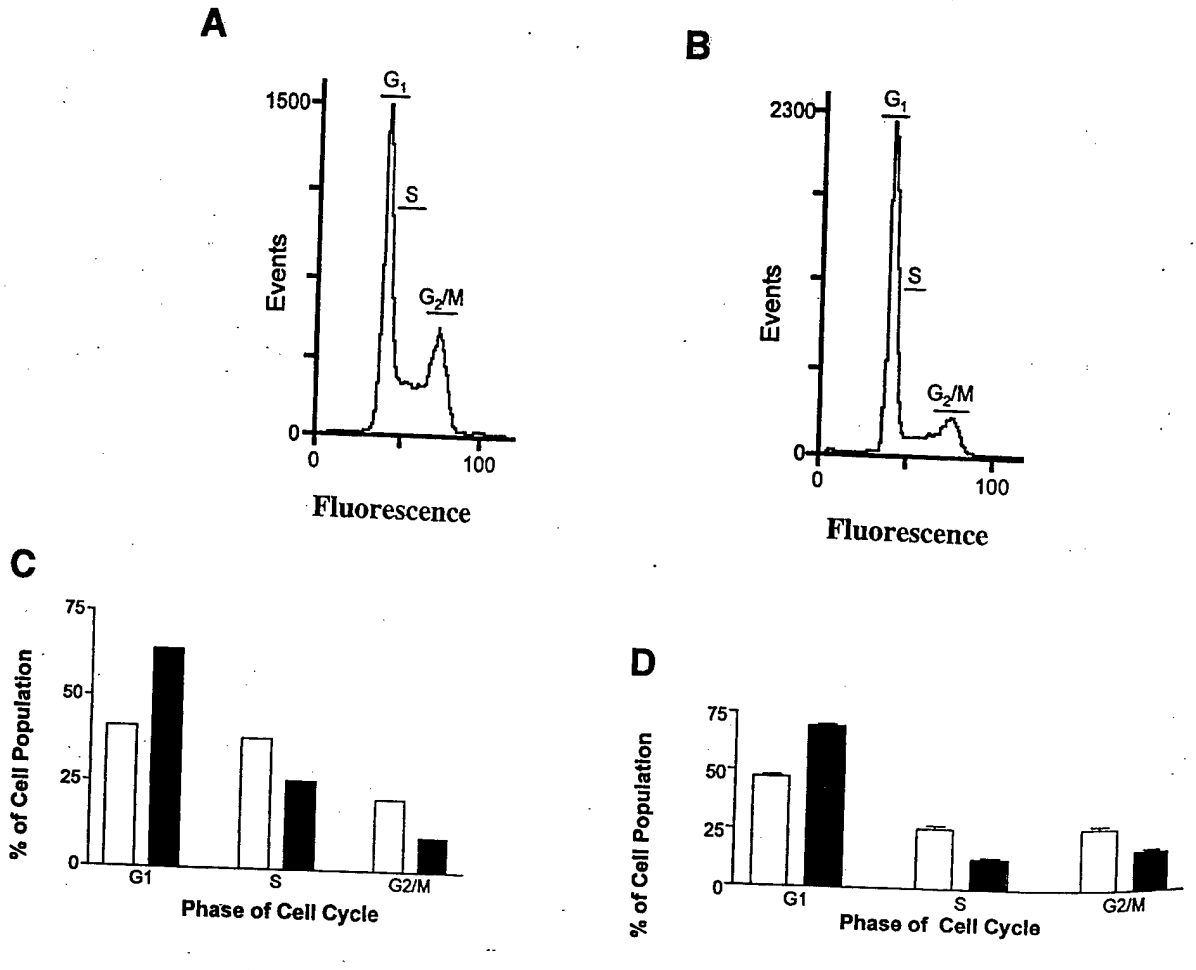
A
1500
G_1
S
G_2/M
Events
0
0
100
Fluorescence
B
2300
G_1
S
G_2/M
Events
0
0
100
Fluorescence
C
75
50
25
0
% of Cell Population
G1
S
G2/M
Phase of Cell Cycle
D
75
50
25
0
% of Cell Population
G1
S
G2/M
Phase of Cell Cycle

Pergamon

Bioorganic & Medicinal Chemistry, Vol. 5, No. 1, pp 165–177, 1997

PII: S0968-0896(96)00199-X
0968-0896/97 $17.00+0.00

Combinatorial Synthesis and Biological Evaluation of Library of Small-Molecule Ser/Thr-Protein Phosphatase Inhibitors

Peter Wipf,[a,*] April Cunningham,[a] Robert L. Rice[b] and John S. Lazo[b,*]
Departments of [a]Chemistry and [b]Pharmacology, University of Pittsburgh, Pittsburgh, PA 15260, U.S.A.

Abstract—In eukaryotes, phosphorylation of serine, threonine, and tyrosine residues on proteins is a fundamental posttranslational regulatory process for such functions as signal transduction, gene transcription, RNA splicing, cellular adhesion, apoptosis, and cell cycle control. Based on functional groups present in natural product serine/threonine protein phosphatase (PSTPase) inhibitors, we have designed pharmacophore model **1** and demonstrated the feasibility of a combinatorial chemistry approach for the preparation of functional analogues of **1**. Preliminary biological testing of 18 structural variants of **1** has identified two compounds with growth inhibitory activity against cultured human breast cancer cells. In vitro inhibition of the PSTPase PP2A was demonstrated with compound **1d**. Using flow cytometry we observed that compound **1f** caused prominent inhibition in the G1 phase of the cell cycle. Thus, the combinatorial modifications of the minimal pharmacophore **1** can generate biologically interesting antiproliferative agents. Copyright © 1997 Elsevier Science Ltd

Introduction

Many eukaryotic cell functions, such as signal transduction, cell adhesion, gene transcription, RNA splicing, apoptosis, and cell proliferation, are controlled by protein phosphorylation, which is regulated by the dynamic relationship between both kinases and phosphatases.[1] Indeed, the principal role of many second messengers is to modulate kinase selectivity. In an effort to intervene early in the initiation stage of cellular events and in recognition of the tumor promoting effects of phorbol ester based protein kinase C activators, the lion's share of synthetic chemistry research in this area has focused on protein kinases.[2] However, there is substantial recent biological evidence for the multiple regulatory functions of protein phosphatases and a clear link between phosphatase inhibition and apoptosis.[3–9]

Besides some minor phosphorylation of histidine, lysine, arginine, and, in bacteria, aspartate, most eukaryotic amino acid phosphate derivatives are found on serine, threonine, and tyrosine protein residues. Generally, the primary characterization of phosphatases follows these structural guidelines: Ser/Thr protein phosphatases (PSTPases), Tyr protein phosphatases (PTPases), and dual-specificity phosphatases (DSPases).[3]

PSTPases have been classified according to their substrate specificity, metal ion dependence and sensitivity to inhibition (Table 1).[10,11] cDNA cloning has revealed at least 40 different enzymes of this type. In addition to proteins (Inhibitor-1, Inhibitor-2, DARPP-32, NIPP-1),[4] several (mostly marine) toxins have been identified as potent inhibitors (Fig. 1).[12]

Okadaic acid is produced by several species of marine dinoflagellates and reversibly inhibits the catalytic subunits of the PSTPase subtypes PP1, PP2A, and PP3.[4] SAR studies showed that the carboxyl group as well as the four hydroxyl groups were important for activity.[13,14] Calyculin A was identified as a cytotoxic component of the marine sponge *Discodermia calyx*. It has an extremely high affinity to PP1, PP2A, and PP3 with an IC_{50} in the 0.3 nM range.[4] Microcystins are potent cyclic hepta- and pentapeptide toxins of the general structure cyclo[D-Ala-X-D-*erythro*-β-methyl-*iso*-Asp-Y-Adda-D-*iso*-Glu-*N*-methyldehydro-Ala] where X and Y are variable L-amino acids.[4] They are known to promote tumors in vivo, but, with the exception of hepatocytes, are impermeable to most cells in vitro.[4]

The large number of naturally occurring microcystins makes it possible to carry out a limited SAR study.[15] Apparent IC_{50}s for microcystins range between 0.05 and 5 nM, with similar preference for PP1, PP2A, and PP3 as found for okadaic acid and calyculin A.[4] The

Table 1. Ser/Thr protein phosphatase classification[3,4]

Family	Subfamily	Characteristic
PSTPases	PP1	IC_{50} for okadaic acid 10–50 nM
	PP2A	IC_{50} for okadaic acid 0.5 nM
	PP2B (calcineurin)	Ca(II)-dependent; IC_{50} for okadaic acid >2000 nM
	PP2C	Mg(II)-dependent; not inhibited by okadaic acid
	PP3	IC_{50} for okadaic acid 4 nM

substitution of alanine for arginine has little effect on phosphatase inhibitory potency; there is, however, a difference in relative cytotoxicity.[15] The dehydroamino acid residue and the *N*-methyl substituents are also not critical. Crucial are the glutamic acid unit, since esterification leads to inactive compounds, and the overall shape of the Adda residue, since the (6Z)-isomer is inactive. Some variations in the Adda unit, specifically the *O*-demethyl and the *O*-demethyl-*O*-acetyl analogues, exert little effect on bioactivity, however. Considerably less information is available in the nodularin series, since fewer compounds are available;

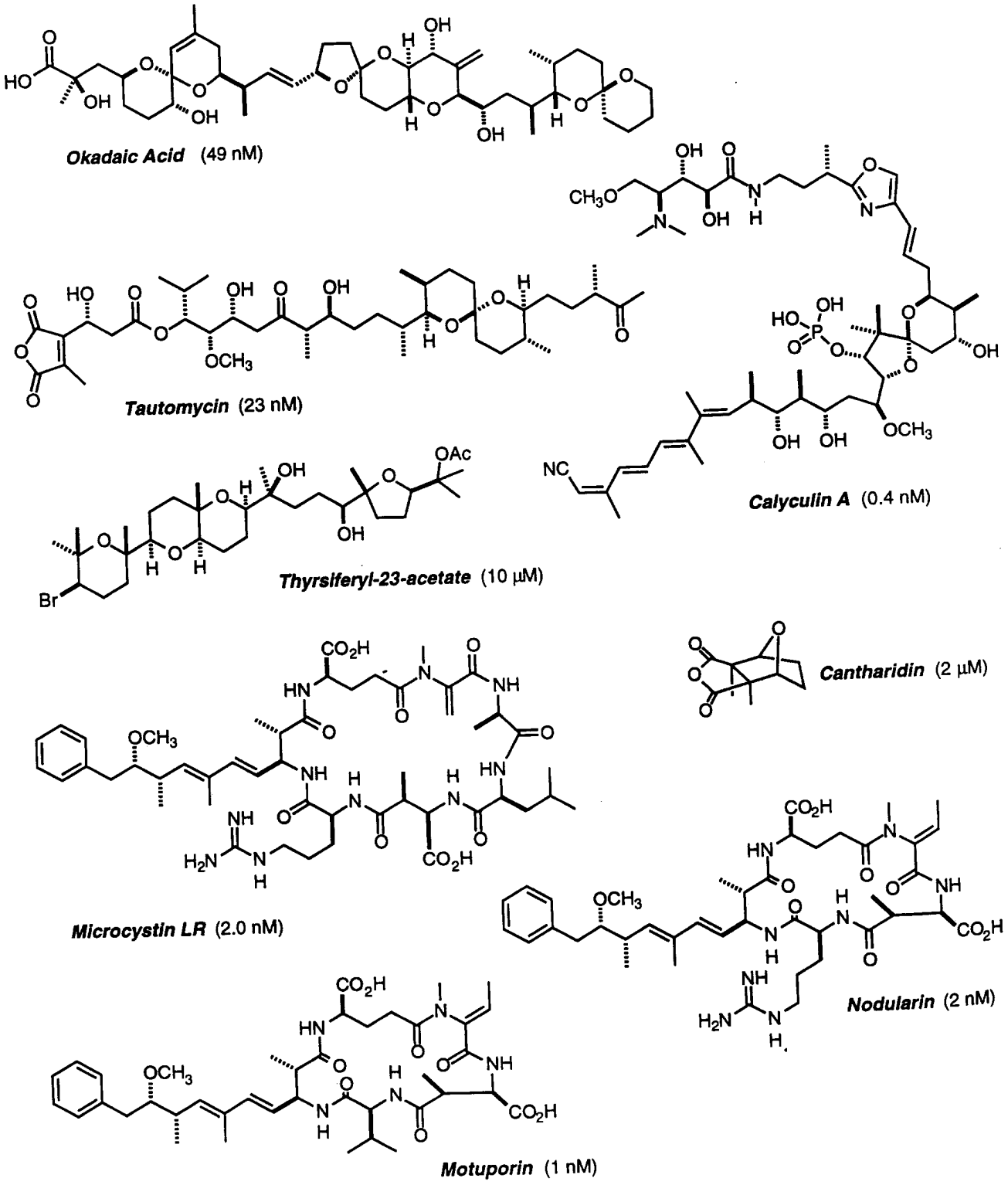

Figure 1. Natural product inhibitors of PSTPases (IC_{50} vs PP1).

however, the general SAR appears similar to the microcystins.[15] There are only slight differences in the inhibition profile; IC_{50}s for PP1 and PP3 are 2 and 1 nM, respectively, which is about 50 times higher than the IC_{50} for PP2A. The recently isolated motuporin (=[L-Val^2]nodularin) is even more potent with an IC_{50} <1 nM for PP1.[16,17] This secondary metabolite was isolated from a Papua New Guinea sponge and is the only member of the greater microcystin family that has thus far yielded to total synthesis.[18]

Tautomycin is produced by a terrestrial *Streptomyces* strain. This relatively unstable molecule inhibits PP1, PP2A and PP3 indiscriminately with an IC_{50} in the 15 nM range.[4] The remaining natural product inhibitors, thyrsiferyl-23-acetate and cantharidine, were shown to be somewhat selective, though weak (IC_{50} 0.16–10 μM) inhibitor of PP2A.[19–22]

Despite some recent total synthesis efforts,[23] no SAR for calyculin A, tautomycin[24] or thyrsiferyl acetate were reported. High toxicity, especially hepatotoxicity, is commonly found with all natural PSTPase inhibitors, often limiting the range of feasible pharmacological studies, and appears to be intrinsically associated with a non-specific phosphatase inhibition.[25] Importantly, based on kinetic and competition binding studies, okadaic acid, calyculin A, tautomycin, and the microcystins appear to bind competitively at the same site of PSTPases.[26–29] Since phosphatases are ubiquitous, precise tools in membrane and post-membrane signal transduction pathways, the development of selective inhibitors or activators of PSTPases that are cell-permeable, non-hepatotoxic, or broadly cytotoxic is of major significance for future progress in this field.

Design and Synthesis of Calyculin A Analogues

The design of our PSTPase inhibitor library was based on the SAR available for the natural product inhibitors and assumed that the presence of a carboxylate, a nonpolar aromatic function, and hydrogen-bond acceptors and donors (e.g. a peptidomimetic group) in suitable spatial arrangements are sufficient for strong and selective binding. A pharmacophore model that addresses these criteria is shown in Figure 2. Traditional computational studies by Quinn *et al.* have identified a related structural model based on molecular modeling of okadaic acid, calyculin A, and microcystin LR.[30] Whereas computational studies of the minimal structural requirements for PSTPase inhibition aim for an accurate prediction of the important conformational and electronic features of the lead structures, our combinatorial[31,32] analysis achieves this goal via a random optimization of the steric and electronic properties of the pharmacophore. Most marine natural products have evolved along an optimization of broad-range activity rather than specificity.[33] The structural variation present in a library of PSTPase inhibitors will allow the simultaneous exploration of high-affinity and high-specificity features providing selectivity beyond the natural product model.

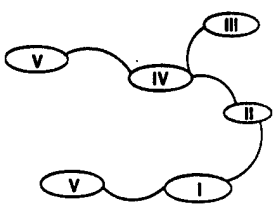

I: H-bond acceptor
II: hydrophobic backbone
III: carboxylic acid, phosphate
IV: H-bond acceptor
V: hydrophobic, extended side-chain

Figure 2. Pharmacophore model for PSTPase inhibitor library.

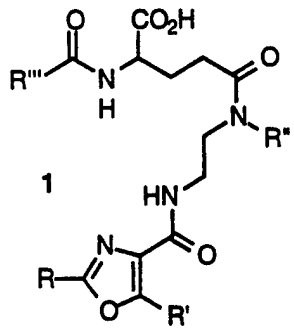

Figure 3. Parent structure for PSTPase inhibitor library synthesis.

Specifically, we have designed compounds of structure **1** to provide a platform for functional group variation according to our pharmacophore model (Fig. 3). The carboxylic acid moiety, crucial for bioactivity, is derived from glutamic acid. The substituent R attached to the oxazole moiety of **1** can be varied within a broad range and should probably be mostly hydrophobic in nature. To a lesser extent, direct substitutions at the oxazole R′ are possible that will explore the tolerance for bulky residues at this site. A variable and relatively flexible diamine segment serves as the spacer between oxazole moiety and carboxylic acid side chain in place of the synthetically less readily accessible spiroketal of calyculin A. A related *N*-methyl dehydroalanine residue is found in microcystin LR. The hydrophobicity of this subunit is modulated by *N*-alkylation with residues R″. An acyl portion R‴CO is responsible for providing the molecule with a relatively rigid hydrophobic tail similar to the Adda amino acid side chain in microcystins and the tetraene cyanide in calyculin A.

Initially, the development of an efficient approach for the combinatorial synthesis of target structures **1** focused on the optimization of the solution-phase synthesis of model compound **2** (Scheme 1). L-Glutamic acid (**3**) was protected in 62% yield as the γ-allyl ester using allyl alcohol and chlorotrimethylsilane.[34] Treatment with Fmoc-Cl followed by coupling to benzyl alcohol using 1-ethyl-3-[3-(dimethylamino-)propyl]-carbodiimide hydrochloride (EDCI) provided the tri-protected amino acid **6** in 82% yield. The Fmoc protective group was subsequently removed by exposure to DMAP and the free amine was acylated in situ with decanoyl chloride to give amide **7** in 63% yield. Pd(0)-catalyzed deprotection[35] of the allyl ester and coupling of the resulting acid **8** to ethylene diamine **9** in the presence of (1H-1,2,3-benzotriazol-1-yloxy)tris(dimethylamino)phosphonium hexafluoro-

phosphate (BOP)[36] led to amide **10** in 75% yield. A versatile general route to monoprotected ethylene diamines was easily achieved by carbamoylation of 2-chloroethylamine monohydrochloride (**12**), Finkelstein reaction, and aminolysis (Scheme 2).

Deprotection of the Alloc-group gave a primary amine which was coupled, in situ, to oxazole acid (**11**) using BOP as a coupling agent. The desired amide **2** was obtained in 57% yield for the two steps. The heterocyclic moiety **11** was efficiently prepared from *N*-benzoyl threonine (**14**) by side-chain oxidation and cyclodehydration with Dess–Martin reagent and electrophilic phosphorus, respectively,[37] followed by saponification of oxazole **15** (Scheme 3).

The solution-phase preparation of calyculin analogue **2** established the necessary general protocols for the preparation of a library of structural variants of the pharmacophore model **1** on solid support. We have successfully applied this basic strategy for the parallel synthesis of 18 structural analogues (Scheme 4, Table 2). Coupling of diprotected glutamate **5** to the polystyrene-based Wang resin[38] with EDCI was performed on large scale and provided a supply of solid phase beads. The base-labile Fmoc protective group was removed by treatment with piperidine and THF, and the resin was distributed to three specially designed Schlenk filters equipped with suction adapters and inert gas inlets for maintaining steady bubbling. After the addition of solvent, hydrophobic residues R'''COCl were added to each flask, which provided three different amide derivatives **17**. After filtration and rinsing of the resin, allyl esters **17** were deprotected via Pd(0) chemistry and each batch was distributed over three modified Schlenk filters, providing nine different reaction sites for acylation. Addition of three different *N*-allyloxycarbonyl protected diamines

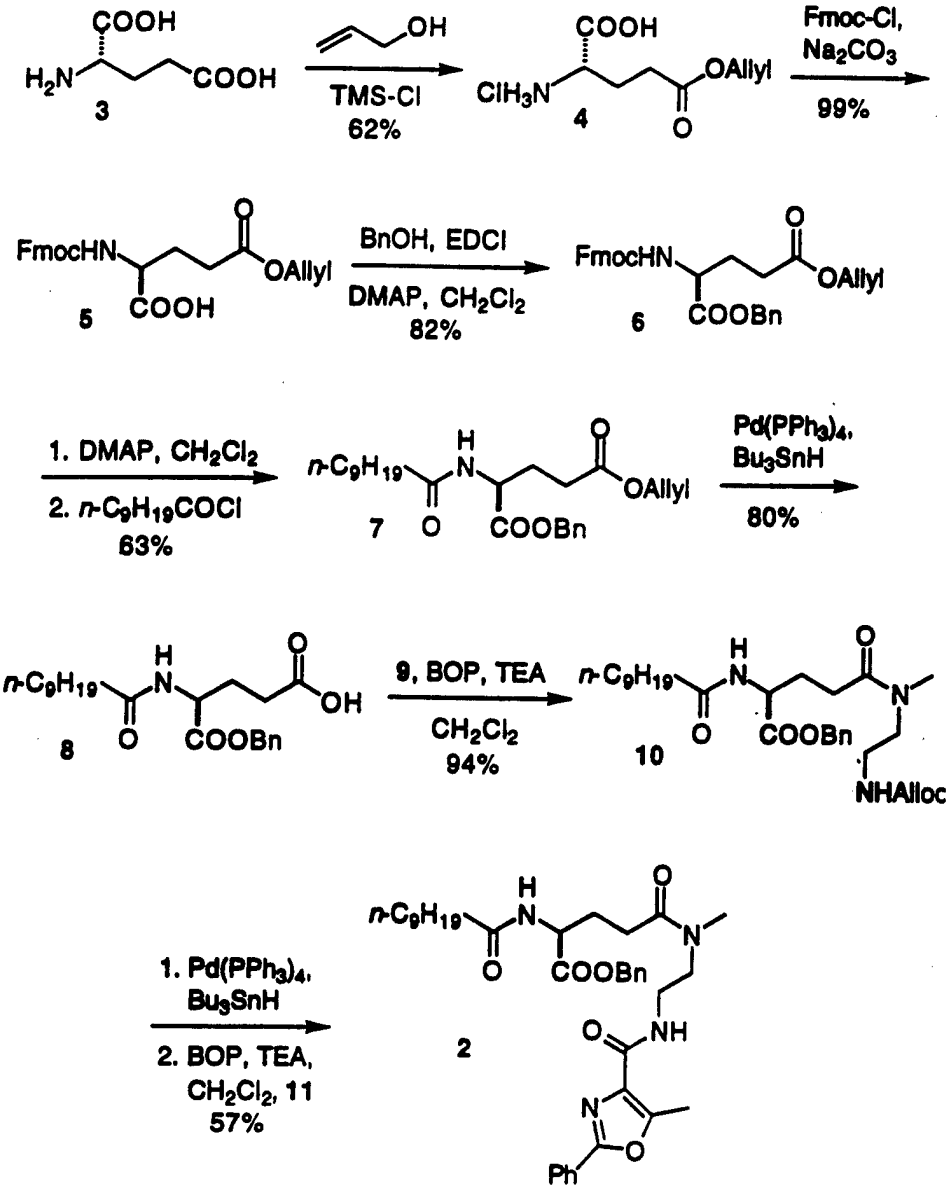

Scheme 1.

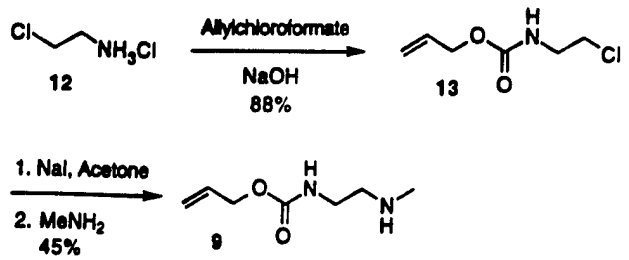

Scheme 2.

in the presence of PyBroP[39] or ClоP[40] as coupling agents extended the side chain carboxyl terminus of glutamic acid toward the desired heterocyclic moiety in **1**. The resulting nine compounds (**18**) were each deprotected at the N-terminus and distributed over two additional Schlenk filters for the final segment condensation. Coupling with two different oxazole carboxylic acids in the presence of ClоP and final purification by rinsing with solvent provided the phosphatase library **1** still attached to the solid support. Complete or partial cleavage with 50% trifluoroacidic acid was necessary to release the carboxylate which is required for biological activity. After filtration of the solid support and evaporation of the resulting mother liquor, the desired compounds **1** were obtained in a chemically pure and structurally well defined fashion ready for rapid throughput biological screening. In each case, the purity of the final compound was >60% according to spectroscopic analysis (^{1}H NMR, MS). The contamination was derived from incomplete couplings to the sterically hindered secondary amine moiety of Alloc-NHCH$_2$CH$_2$NH(R^a). A small sample of resin had been routinely cleaved for reaction monitoring, but this coupling was difficult to drive to completion. Mass recovery was essentially quantitative. We are still in the process of further optimizing the reaction sequence and are confident that purities of >80% for the final material **1** can routinely be achieved after improvement of the coupling step.

Preliminary Biochemical and Biological Analysis of Library 1

We have begun to evaluate the ability of compounds **1a–r** to inhibit PP1 and PP2A. Initial studies were conducted in collaboration with Drs A. Boynton and D. Messner.[41] with their previously described assay.[25,29] These preliminary studies demonstrated that several members of our library inhibit protein phosphatases PP1 or PP2A by >50% at concentrations of 100 μM. We have further examined the ability of one member of the library to inhibit the catalytic activity of PP2A. As demonstrated in Figure 4, calyculin A inhibited PP2A activity at 10 nM, and compound **1d** caused 50% inhibition at 100 μM. These results document that our minimal structure retained the ability to inhibit the catalytic activity of Ser/Thr phosphatase. More comprehensive analyses are currently being conducted.

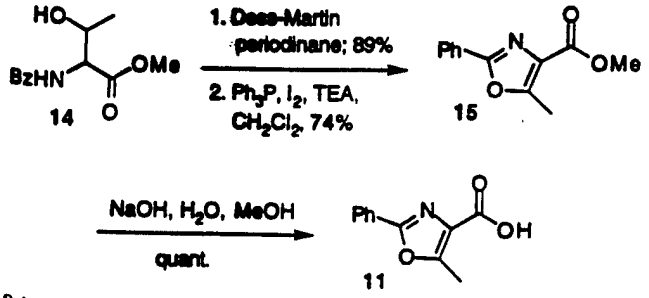

Scheme 3.

PSTPases are intracellular targets and, thus, we have examined the antiproliferative effects of members of the library to indirectly assess whether our compounds might enter cells. Exponentially growing human MDA-MB-231 breast carcinoma cells were exposed to all compounds at the highest available concentrations, which ranged from 30 to 100 μM. With the exception of two compounds, all lacked significant growth inhibitory activity. Compound **1i** caused 50% growth inhibition at 20 μM but had no further cytotoxicity at higher drug concentrations. Compound **1f** caused 50% growth inhibition at 100 μM and had a clear concentration-dependency (Fig. 5). Cell proliferation is coordinated by phosphorylation of cyclin-dependent kinases and tightly regulated by both kinases and phosphatases.[42] Thus, inhibition of Ser/Thr phosphatases such as PP2A or PP1 can result in disrupted cell cycle transition with restriction at discrete points in the cell cycle. Exponentially growing human MDA-MB-231 breast cancer cell populations (population doubling time of approximately 30–35 h) typically have approximately 50% of all cells in the S or DNA synthetic phase of the cell cycle (Fig. 6A,C). In contrast, when MDA-MB-231 cells were incubated for 48 h with 88 μM compound **1f**, there was prominent accumulation in the G1 phase with a concomitant decrease in both S and G2/M phases (Fig. 6B,C). Incubation of MDA-MB-231 cells for 72 h with 88 μM **1f** also caused a prominent accumulation in the G1 phase (Fig. 6D).

Discussion

Due to the limited character of previous SAR studies of the available natural product serine/threonine phosphatase inhibitors, the design of a small-molecule pharmacophore model has to allow for considerable structural variation. The combinatorial chemistry strategy is therefore ideally suited to address this problem. Among the characteristic structural features of calyculin A and the microcystins, the presence of a carboxylate, amide, oxazole, and lipophilic moieties are important features shared with our first generation lead structure **1**. The use of traditional amide coupling protocols combined with transition metal susceptible protective groups provided the basis for the parallel synthesis of 18 analogues of **1** via a solid-phase chemistry. We have begun to test this library both for biochemical and biological activity. Figure 4 demonstrates that the basic pharmacophore that we have

identified retains the ability to inhibit Ser/Thr phosphatases. We have not yet evaluated other members of our library with this assay, but inhibition of PP2A and PP1 has been established in preliminary studies for several members of our library. Compounds **1a–r** were further subjected to an assay for cytotoxicity and apoptosis in human breast carcinoma cells, and two members (**1h** and **f**) with an IC_{50} of <100 μM were found.[43] Interestingly, **1d**, which can block PP2A activity did not appear to be cytotoxic. This lack of biological activity may be due to poor cell penetration of cellular metabolism. Compound **1h** did not suppress cell proliferation significantly more than 50% in our assay and thus was not examined further. Compound **1f**, however, exhibited a concentration-dependent inhibition in proliferation of MDA-MB-231 cells and flow cytometry data confirmed blockage in cell cycle progression at the G1 checkpoint. Although PSTPase inhibitors such as okadaic acid and calyculin A often are found to block cells in G2/M, a concentration-depended cell cycle arrest at the G1/S interface similar to that seen by us has been detected with some cells.[44] An additional attractive target

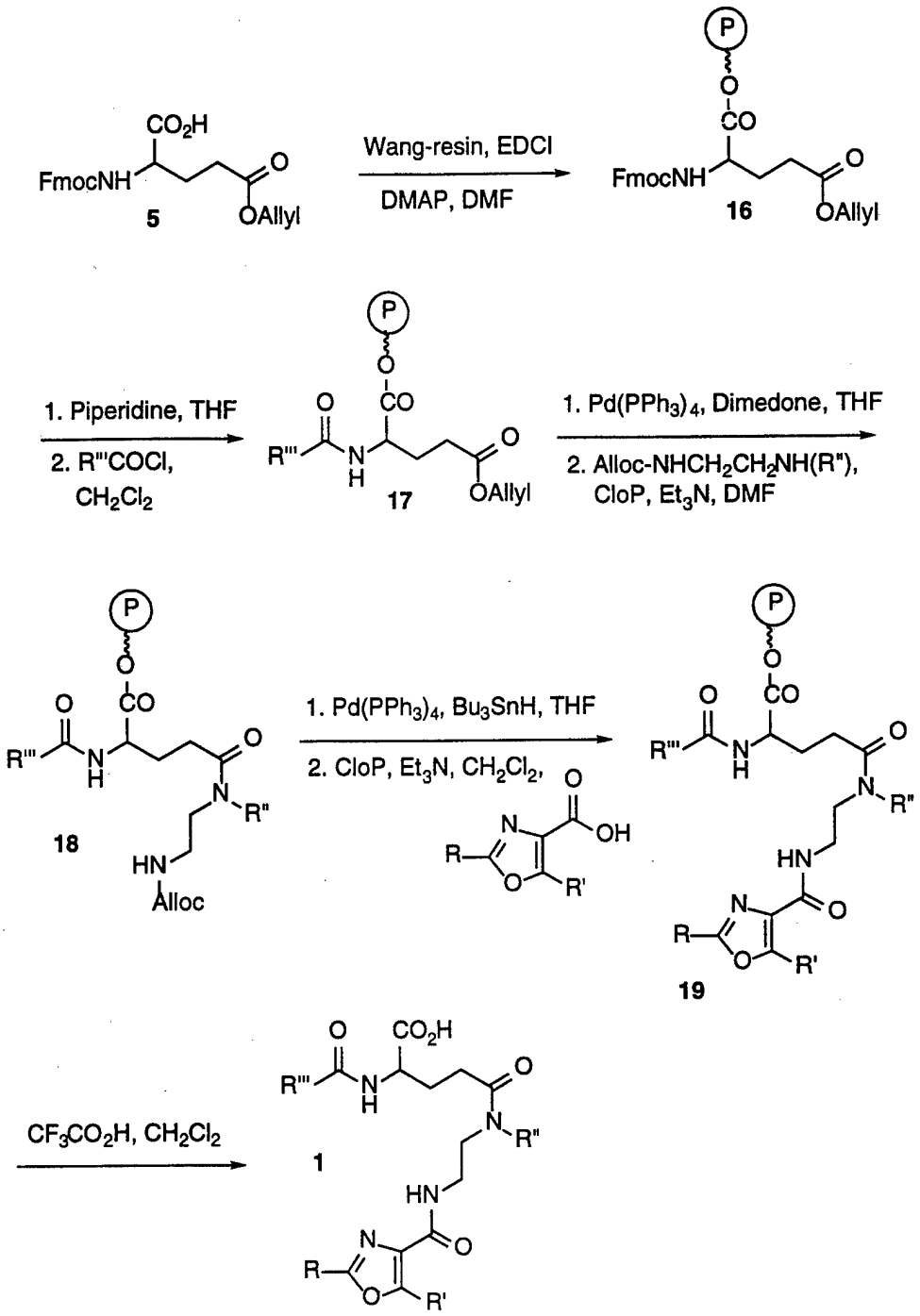

Scheme 4.

Table 2. Test library of 18 structural variants of pharmacophore model 1 prepared according to *Scheme 4*

Compound	R	R′	R″	R‴
1a	Ph	CH_3	CH_3	n-C_9H_{19}
1b	Ph	CH_3	n-C_6H_{13}	n-C_9H_{19}
1c	Ph	CH_3	Bn	n-C_9H_{19}
1d	Ph	Ph	CH_3	n-C_9H_{19}
1e	Ph	Ph	n-C_6H_{13}	n-C_9H_{19}
1f	Ph	Ph	Bn	n-C_9H_{19}
1g	Ph	CH_3	CH_3	$PhCH_2CH_2$
1h	Ph	CH_3	n-C_6H_{13}	$PhCH_2CH_2$
1i	Ph	CH_3	Bn	$PhCH_2CH_2$
1j	Ph	Ph	CH_3	$PhCH_2CH_2$
1k	Ph	Ph	n-C_6H_{13}	$PhCH_2CH_2$
1l	Ph	Ph	Bn	$PhCH_2CH_2$
1m	Ph	CH_3	CH_3	PhCH=CH
1n	Ph	CH_3	n-C_6H_{13}	PhCH=CH
1o	Ph	CH_3	Bn	PhCH=CH
1p	Ph	Ph	CH_3	PhCH=CH
1q	Ph	Ph	n-C_6H_{13}	PhCH=CH
1r	Ph	Ph	Bn	PhCH=CH

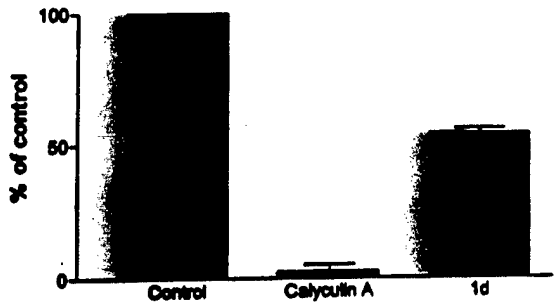

Figure 4. Inhibition of PP2A activity by compound 1d. The catalytic subunit of PP2A was incubated with vehicle alone (control), calyculin A (10 nM), or **1d** (100 μM), and the dephosphorylation of the substrate fluorescein diphosphate determined spectrofluorometrically. Mean results to two independent experiments are shown; bars indicate the range.

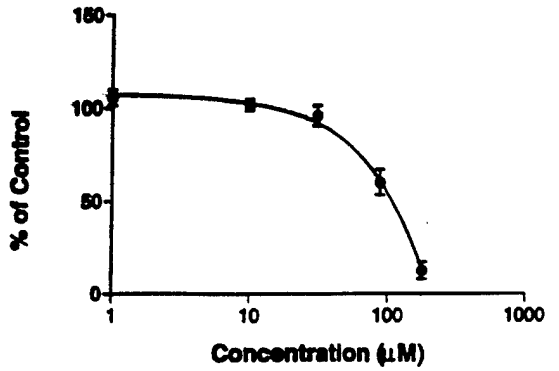

Figure 5. Antiproliferative effect of compound **1f** against human MDA-MB-231 breast cancer cells.

phosphatase that might control the G1/S transtion would be the dual specificity phophatase cdc25A.[45] Studies of the effect of **1a–r** on cdc25A and other phosphatases that may control cell cycle checkpoints are currently in progress.

These results clearly demonstrate the feasibility of using a combinatorial approach based on a natural product lead to identify novel antiproliferative and potential antineoplastic agents. Since cellular signal transduction is regulated by reversible enzymatic phosphorylation of serine, threonine and tyrosine residues on proteins, we expect that appropriately substituted, phosphatase-specific isomers of **1** will become important probes for transcription factor regulation, cell cycle control, and membrane and post-membrane signaling pathways. We are actively pursuing the synthesis and rapid-screening assays of much larger libraries based on **1** to identify more potent and more specific analogues.

Experimental Section

General methods

All glassware was dried in an oven at 150 °C prior to use. THF and dioxane were dried by distillation over Na/benzophenone under a nitrogen atmosphere. Dry CH_2Cl_2, DMF and CH_3CN were obtained by distillation from CaH_2.

2-Amino-pentanedioic acid 5-allyl ester (4). To a stirred suspension of 2.5 g (16.9 mmol) of L-glutamic acid (**3**) in 40 mL of dry allyl alcohol was added dropwise 5.4 mL (42.3 mmol) of chlorotrimethylsilane. The suspension was stirred at 22 °C for 18 h and poured into 300 mL of Et_2O. The resulting white solid was filtered off, washed with Et_2O, and dried in vacuo to provide 3.80 g (62%) of **4**: mp 133–134.5 °C (Et_2O); IR (KBr) 3152, 2972, 2557, 1738, 1607, 1489, 1450, 1289, 1366, 1264, 1223, 1177, 1146, 1121, 1084 cm^{-1}; ^1H NMR (D_2O): δ 5.8–5.7 (m, 1 H), 5.14 (dd, 1 H, J = 1.4, 17.3 Hz), 5.09 (dd, 1 H, J = 1.0, 10.4 Hz), 4.44 (d, 2 H, J = 5.6 Hz), 3.92 (t, 1 H, J = 6.8 Hz), 2.48 (t, 2 H, J = 7.0 Hz), 2.1–2.0 (m, 2 H); ^{13}C NMR (DMSO-d_6): δ 171.5, 170.6, 132.7, 117.9, 64.7, 51.2, 29.3, 25.2; MS (EI) *m/z* (relative intensity) 188 (63), 142 (72), 128 (27), 100 (21), 85 (100), 74 (32), 56 (73).

2-(9-H-Fluoren-9-ylmethoxycarbonlyamino)-pentanedioic acid 5-allyl ester (5). To 20 mL of dioxane was added 1.5 g (6.7 mmol) of ester **4**. The resulting suspension was treated with 16.8 mmol (17.7 mL of a 10% soln) of Na_2CO_3 at 0 °C, stirred for 5 min and treated with 1.74 g (6.7 mmol) of Fmoc-Cl dissolved in 10 mL of dioxane. The reaction mixture was warmed to 22 °C, stirred for 3 h, poured into 50 mL of H_2O and extracted with Et_2O (2 × 25 mL). The aq layer was cooled to 0 °C, acidified to pH 1 with conc HCl, and extracted with EtOAc (3 × 25 mL). The resulting organic layer was dried (Na_2SO_4) and concd in vacuo to give 2.72 g (99%) of **5** as a viscous oil: $[\alpha]_D$ +8.5° (*c*

2.8, $CHCl_3$, 21 °C); IR (neat) 3312, 3061, 2951, 2361, 2349, 2332, 1725, 1528,1447, 1414, 1325, 1254, 1117, 1078, 1049 cm^{-1}; ^1H NMR: δ 11.09 (br s, 1 H), 7.73 (d, 2H, J= 7.5 Hz), 7.57 (d, 2H, J=5.1 Hz), 7.4–7.25 (m, 4H), 6.0–5.85 (m, 1 H), 5.76 (d, 1H, J=8.1 Hz), 5.30 (d, 1H, J=19.5 Hz), 5.21 (d, 1H, J=10.5 Hz), 4.6–4.35 (m, 5H), 4.19 (t, 1H, J=6.6 Hz), 2.5–2.2 (m, 4H); ^{13}C NMR: δ175.6, 172.6, 156.2, 143.7, 143.5, 141.2, 131.7, 127.6, 127.0, 125.0, 119.9, 118.4, 67.1, 65.4, 53.1, 46.9, 30.2, 27.1; MS (EI) *m/e* (rel. int.) 409 (7), 351 (19), 338 (12), 280 (11), 239 (11), 196 (12), 178 (100), 165 (40); HRMS (EI) calcd for $C_{23}H_{23}NO_6$: 409.1525, found: 409.1501.

2-(9H-Fluoren-9-ylmethoxycarbonylamino)-pentanedioic acid 5-allyl ester 1-benzyl ester (6). To a soln of 1.5 g (36.6 mmol) of **5** in 5 mL of CH_2Cl_2 was added 0.42 mL (40.3 mmol) of benzyl alcohol, 0.912 g (47.6 mmol) of EDCI, and 45 mg (3.66 mmol) of dimethylaminopyridine (DMAP). The reaction mixture was stirred at 22 °C for 6 h, diluted with 20 mL of CH_2Cl_2, and extracted with H_2O (1 × 15 mL), 0.1 M HCl (2 × 15 mL), and brine (2 × 10 mL). The organic layer was dried (Na_2SO_4), concd in vacuo, and chromatographed on SiO_2 (hexanes:EtOAc, 5:1) to give 1.83 g (82%) of **6** as a white solid: mp 66.2–67.1 °C (EtOAc:hexanes); $[\alpha]_D$ +1.4° (*c* 1.64, $CHCl_3$, 21 °C); IR (neat) 3314, 1726, 1682, 1527, 1443, 1414, 1383, 1254, 1173, 1099, 1082, 980, 754, 735 cm^{-1}; ^1H NMR: δ 7.75 (d, 2 H, J=7.4 Hz), 7.59 (d, 2H, J=7.1 Hz), 7.41–7.27 (m, 9H), 5.95–5.85 (m, 1H), 5.44 (d, 1H, J=8.2 Hz), 5.34–5.19 (m, 4H), 4.56 (d, 2H, J=5.6 Hz), 4.5–4.4 (m, 3H), 4.21 (t, 1H, J=7.0 Hz), 2.5–2.0 (m, 4H); ^{13}C NMR: δ 172.2, 171.6, 155.8, 143.7, 143.5, 141.1, 135.0, 131.8, 128.5, 128.3, 128.1, 127.6, 126.9, 124.9, 119.8, 118.3, 67.2, 66.9, 66.2, 53.3, 47.0, 28.0, 27.3; MS (FAB, MNBA/MeOH) *m/z* (rel. int.) 500 ($[M+H]^+$, 40), 465 (8), 448 (14), 433 (12), 413 (8), 386 (38), 371 (24), 349 (9), 324 (16), 309 (26), 293 (11), 265 (10), 247 (24), 231 (56), 215 (39), 202 (26), 191 (24), 179 (67), 165 (48), 154 (67), 143 (31), 133 (71), 117 (100).

2-Decanoylamino-pentanedioic acid 5-allyl ester 1-benzyl ester (7). To a suspension of 1 g (2.0 mmol) of **6** in 10 mL of CH_2Cl_2 was added 1 g (8.2 mmol) of DMAP. The reaction mixture was stirred at 22 °C for

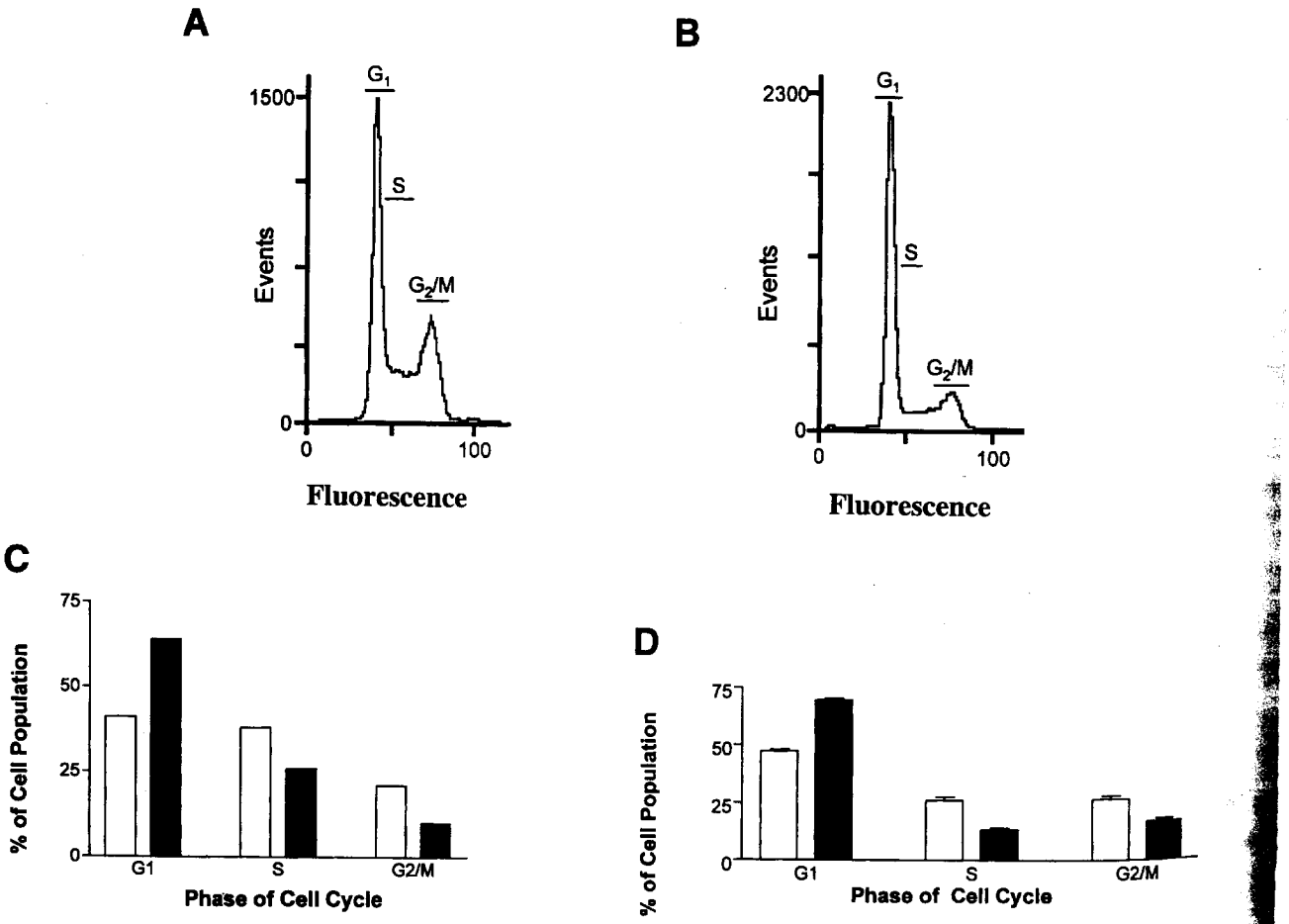

Figure 6. Cell cycle distribution of human breast cancer cells after treatment with compound **1f** determined by flow cytometry. Panel A. Flow cytometry analysis of MDA-MB-231 cells treated with vehicle alone. Panel B. Flow cytometry analysis 48 h after treatment with 88 μM compound **1f**. Fluorescence channel measures intracellular propidium iodide concentration, an index of DNA content. Horizontal bars are the gating positions that allow for cell cycle analysis. Panel C. MDA-MB-231 cell cycle distribution 48 h after continuous treatment with 88 μM compound **1f**. This is the result of one experiment. Open bars are control cells and black bars are cells treated with **1f**. Panel D. Cell cycle distribution 72 h after continuous treatment with 88 μM **1f**. The mean values were obtained from three independent determinations. Open bars are control cells and black bars are cells treated with 88 μM **1f**. The SE of the mean are displayed.

24 h, treated with 0.62 mL (3.0 mmol) of decanoyl chloride, stirred for 2 h at 22 °C, and extracted with satd Na_2CO_3 (2 × 10 mL). The organic layer was dried (Na_2SO_4), evapd to dryness, and the residue was chromatographed on SiO_2 (hexanes:EtOAc, 5:1) to give 548 mg (63%) of **7** as a viscous oil: IR (neat) 3293, 3063, 2924, 2855, 1740, 1649, 1534, 1453, 1379, 1175, 986, 930 cm^{-1}; ^1H NMR: δ 7.26 (s, 5H), 6.68 (d, 1H, J = 7.8 Hz), 5.85–5.75 (m, 1H), 5.22 (d, 1H, J = 17.3 Hz), 5.14 (d, 1H, J = 10.4 Hz), 5.08 (s, 2H), 4.63–4.57 (m, 1H), 4.48 (d, 2H, J = 5.6 Hz), 2.38–2.28 (m, 2H), 2.2–2.1 (m, 3H), 2.0–1.9 (m, 1H), 1.55 (t, 2H, J = 6.9 Hz), 1.20 (bs, 12H), 0.82 (t, 3 H, J = 5.9 Hz); ^{13}C NMR δ 173.0, 172.1, 171.6, 135.0, 131.7, 128.2, 128.1, 127.8, 117.9, 66.8, 64.9, 51.3, 36.0, 31.6, 29.9, 29.1, 29.0, 26.8, 25.3, 22.3, 13.8; MS (EI) *m/z* (rel. int.) 431 (12), 319 (21), 296 (51), 142 (100), 124 (31), 91 (91); HRMS (EI) *m/z* calcd for $C_{25}H_{37}NO_5$: 431.2672, found: 431.2673.

2-Decanoylamino-pentanedioic acid 1-benzyl ester (8). To a soln of 752 mg (1.74 mmol) of 2-decanoylamino-pentanedioic acid **7** in 10 mL of CH_2Cl_2 was added 100 mg (0.087 mmol) of tetrakistriphenylphosphine Pd(0) followed by 0.52 mL (1.9 mmol) of tributyltin hydride. After 15 min, the reaction mixture was quenched with 10 mL of a 10% HCl soln. The aq layer was reextracted with 15 mL of CH_2Cl_2 and the organic layer dried (Na_2SO_4), concd in vacuo, and chromatographed on SiO_2 (hexanes:EtOAc, 9:1) to provide 545 mg (79.9%) of **8** as a thick oil: $[\alpha]_D$ +2.8° (*c* 1.2, $CHCl_3$, 21 °C); IR (neat) 3351, 3064, 2995, 2852, 1738, 1712, 1657, 1536, 1454, 1380, 1364, 1265, 1209, 1183, 1121, 739 cm^{-1}; ^1H NMR: δ 10.9–10.7 (br s, 1 H), 7.22 (s, 5 H), 6.58 (d, 1H, J = 7.8 Hz), 5.09 (s, 2H), 4.63 (dd, 1H, J = 8.1, 12.9 Hz), 2.4–2.25 (m, 2H), 2.2–2.1 (m, 3H), 2.0–1.9 (m, 1H), (m, 6H), 1.53 (t, 2H, J = 6.6 Hz), 1.19 (br s, 12H), 0.81 (t, 3H, J = 6.0 Hz); ^{13}C NMR: δ 176.9, 174.0, 171.8, 134.9, 128.5, 128.4, 128.1, 67.3, 51.4, 36.2, 31.7, 29.9, 29.3, 29.2, 29.1, 27.0, 25.5, 22.5, 14.0; MS (EI) *m/z* (rel. int.) 391 (54), 373 (62), 279 (13), 256 (19), 178 (27), 178 (23), 155 (13), 146 (6), 130 (7), 102 (100); HRMS (EI) *m/z* calcd for $C_{22}H_{33}NO_5$: 391.2358, found: 391.2350.

4-[(2-Allyloxycarbonylamino-ethyl)-methyl-carbamoyl]-2-decanoylamino-butyric acid benzyl ester (10). To a soln of 526 mg (1.3 mmol) of **8** in 10 mL of CH_2Cl_2 was added 225 μL (1.61 mmol) of triethylamine and 320 mg (2.0 mmol) of secondary amine **9**. The solution was stirred at 22 °C for 5 min, treated with 710 mg (1.61 mmol) of benzotriazol-1-yloxy-tris(dimethylamino)-phosphonium hexafluorophosphate (BOP reagent), stirred at 22 °C for 10 min, concd in vacuo, dissolved in 15 mL of EtOAc, and extracted with 2 M HCl soln. The organic layer was chromatographed on SiO_2 (hexanes:EtOAC, 1:3) to give 715 mg (94%) of **10** as a clear oil: $[\alpha]_D$ +5.3 (*c* 0.58, $CHCl_3$, 21 °C); IR (neat) 3420, 3250, 2924, 1713, 1680, 1657, 1642, 1632, 1537, 1495, 1470, 1455, 1252, 845 cm^{-1}; ^1H NMR: δ 7.35–7.2 (br s, 5 H), 6.97 (d, 0.3H, J = 7.5 Hz), 6.82 (d, 0.7 H, J = 7.3 Hz), 5.9–5.6 (m, 2H), 5.3–5.1 (m, 4H), 4.65–4.5 (m, 1H), 4.50 (d, 2H, J = 4.9 Hz); 3.55 (t, 1H, J = 7.0 Hz), 3.35–3.1 (m, 3H), 2.85 (s, 3H), 2.4–1.8 (m, 6H), 1.65–1.5 (m, 2H), 1.22 (bs, 12H), 0.84 (t, 3H, J = 6.1 Hz); ^{13}C NMR (MeOD): δ 176.4, 176.3, 174.4, 174.2, 173.2, 158.6, 137.1, 134.3, 134.2, 132.9, 129.5, 129.2, 129.1, 117.6, 117.4, 67.8, 66.3, 66.2, 53.5, 53.3, 39.6, 39.3, 36.7, 36.6, 34.2, 32.9, 30.5, 30.4, 30.3, 30.2, 29.7, 27.6, 26.8, 23.6, 14.5; MS (EI) *m/z* (rel. int.) 531 (16), 473 (37), 418 (16), 396 (26), 374 (38), 361 (17), 338 (87), 220 (54), 184 (52), 155 (36), 130 (29), 101 (37), 91 (100); HRMS (EI) *m/z* calcd for $C_{29}H_{45}N_3O_6$: 531.3308, found: 531.3316.

2-Decanoylamino-4-(methyl-{3-[5-methyl-2-phenyl-oxazole-4-carbonyl]-ethyl}-carbamoyl)-butyric acid benzyl ester (2). To a soln of 193 mg (0.363 mmol) of **10** in 15 mL of CH_2Cl_2 was added 20 mg (0.018 mmol) of tetrakistriphenylphosphine Pd(0), 127 μL (0.472 mmol) of tributyltin hydride, and 20 μL of H_2O. The reaction mixture was stirred at 22 °C for 5 min, filtered through a plug of basic Al_2O_3 and treated with 150 mg (0.726 mmol) of oxazole **11**, 60 mL (0.436 mmol) of triethylamine, and 192 mg (0.436 mmol) of BOP reagent. The reaction mixture was stirred for 30 min at 22 °C, diluted with 10 mL of CH_2Cl_2, and extracted with satd $NaHCO_3$ soln, 1 M HCl, and brine. The organic layer was concd in vacuo and chromatographed on SiO_2 (hexanes:EtOAc, 1:1) to give 131 mg (57%) of **2** as a viscous oil: $[\alpha]_D$ −0.8° (*c* 1.32, $CHCl_3$, 21 °C); IR (neat) 3476, 3415, 3311, 3065, 2925, 2854, 1741, 1649, 1526, 1491, 1379, 1338, 1264, 1240, 1200, 1174, 1070, 711 cm^{-1}; ^1H NMR: δ 8.0–7.95 (m, 2H), 7.5–7.4 (m, 2H), 7.33 (br s, 6 H), 6.93 (d, 0.3H, J = 7.0 Hz), 6.85 (d, 0.7H, J = 7.2 Hz), 5.18–5.07 (m, 2H), 4.65–4.55 (m, 1H), 3.7–3.3 (m, 4H), 2.98 (s, 1H), 2.96 (s, 2H), 2.71 (d, 3H, J = 2.6 Hz), 2.6–2.0 (m, 6H), 1.58 (t, 2H, J = 6.8 Hz), 1.3–1.1 (br s, 12H), 0.86 (t, 3H, J = 6.9 Hz); ^{13}C NMR: δ 173.3, 172.8, 172.0, 171.9, 182.5, 158.6, 153.2, 152.8, 135.9, 130.7, 130.6, 129.7, 128.8, 128.5, 128.3, 128.2, 126.7, 126.5, 126.2, 66.9, 52.2, 52.1, 48.9, 47.6, 37.2, 37.1, 36.4, 36.3, 36.2, 34.1, 31.8, 29.6, 29.5, 29.4, 29.3, 29.2, 28.9, 26.8, 26.6, 25.5, 22.8, 14.1, 11.8; MS (EI) *m/z* (rel. int.) 632 (38), 497 (9), 405 (18), 374 (22), 260(21), 220 (42), 186 (56), 105 (18), 91 (100); HRMS calcd for $C_{36}H_{48}N_4O_6$: 632.3574, found: 632.3572.

(2-Chloro-ethyl)-carbamic acid allyl ester (13). A soln of 2.5 g (22 mmol) of chloroethylamine hydrochloride in 10 mL of 6 M NaOH was cooled to 0 °C and treated dropwise with 2.7 mL (25.9 mmol) of allyl chloroformate while keeping the pH at 9 by addition of 6 M NaOH soln. The reaction was then warmed to 22 °C, stirred for 2 h, and extracted with THF. The organic layer was dried (Na_2SO_4), concd in vacuo, and chromatographed on SiO_2 (hexanes:EtOAc, 9:1) to give 3.1 g (88%) of **13** as a yellow oil: IR (neat) 3333, 2949, 2348, 1705, 1647, 1529, 1433, 1368, 1248, 1190, 1144, 1061, 991, 929, 776 cm^{-1}; ^1H NMR: δ 6.05–5.85 (m, 1H), 5.55–5.35 (br s, 1H), 5.26 (dd, 1H, J = 1.5, 17.1 Hz), 5.18 (dd, 1H, J = 1.0, 10.4), 4.54 (d, 2H, J = 5.5 Hz), 3.57 (t, 2H, J = 5.5 Hz), 3.5–3.35 (m, 2H); ^{13}C NMR: δ 156.0, 132.5, 117.7, 65.6, 43.8, 42.7.

(2-Methylamino-ethyl)-carbamic acid allyl ester (9). A soln of 14 g (86 mmol) of **13** and 25 g (172 mmol) of NaI in 40 mL of acetone was refluxed for 18 h, concd in vacuo, dissolved in H_2O, and extracted with CH_2Cl_2. The organic layer was dried (Na_2SO_4) and cooled to 0 °C. Methyl amine was bubbled through the reaction mixture until the solution was satd. The reaction mixture was warmed to 22 °C, stirred for 36 h, concd in vacuo and chromatographed on SiO_2 (EtOAc) to produce 6.14 g (45%) of **9** as a yellow oil: IR (neat) 3306, 2938, 2313, 1844, 1703, 1651, 1525, 1460, 1383, 1256, 1144, 995, 927, 775 cm^{-1}; ^1H NMR: δ 5.95–5.8 (m, 1 H), 5.28 (dd, 1H, J=1.4, 17.3 Hz), 5.18 (d, 1H, J=10.4 Hz), 4.54 (d, 2H, J=5.3 Hz), 4.9–4.6 (br s, 1 H), 3.34 (q, 2H, J=5.6 Hz), 2.79 (t, 2H, J=5.6 Hz), 2.47 (s, 3H); ^{13}C NMR: δ 157.2, 132.8, 117.6, 65.5, 50.7, 39.7, 35.4; MS (EI) *m/e* (rel. int.) 158 (32), 138 (17), 129 (25), 101 (13), 84 (12), 73 (13), 57 (100).

5-Methyl-2-phenyl-oxazole-4-carboxylic acid methyl ester (15). A soln of 750 mg (3.2 mmol) of **14** in 10 mL of CH_2Cl_2 was treated with 1.61g (3.8 mmol) of Dess–Martin reagent. The reaction was stirred at 22 °C for 10 min, concd in vacuo, and chromatographed on SiO_2 (hexanes:EtOAc, 3:2) to give 658 mg (89%) of 2-benzoylamino-3-oxo-butyric acid methyl ester. Alternatively, a soln of 9.12 g (38 mmol) of **14** in 80 mL of CH_2Cl_2 was cooled to −23 °C and treated with 16.1 mL (115 mmol) of triethylamine and a soln of 18.3 g (115 mmol) of SO_3–pyridine complex in 60 mL of dry DMSO. The reaction mixture was warmed to 22 °C, stirred for 30 min, then cooled to −48 °C and quenched with 20 mL of satd $NaHCO_3$. The soln was extracted with 50 mL of hexanes:EtOAc (2:1). The aq layer was reextracted with hexanes:Et_2O (2:1) and the combined organic layers were washed with brine, dried (Na_2SO_4), and chromatographed (hexanes:EtOAc, 3:2) to give 7.1 g (79%) of 2-benzoylamino-3-oxo-butyric acid methyl ester as a white solid: mp 112.7–113.3 °C (hexanes:EtOAc); IR (neat) 3402, 1734, 1662, 1599, 1578, 1510, 1478, 1435, 1354, 1269, 1156, 1121, 912, 804, 714 cm^{-1}; ^1H NMR: δ 8.2–8.1 (br s, 1H), 8.0–7.4 (m, 5H), 5.49 (s, 1H), 3.86 (s, 3H), 2.33 (s, 3H); ^{13}C NMR: δ 168.2, 167.2, 132.6, 132.5, 132.1, 128.7, 127.3, 83.9, 54.2, 23.2; MS (EI) *m/e* (rel. int.) 235 (13), 208 (18), 192 (8), 121 (7), 105 (100), 77 (58).

A soln of 277 mg (1.06 mmol) of triphenylphosphine, 268 mg (1.06 mmol) of iodine, and 0.29 mL (2.11 mmol) of triethylamine in 5 mL of CH_2Cl_2 was cooled to −48 °C and treated with a soln of 124 mg (0.528 mmol) of 2-benzoylamino-3-oxo-butyric acid methyl ester in 5 mL of CH_2Cl_2. The reaction mixture was warmed to 22 °C, stirred for 20 min, transferred to a separatory funnel and extracted with aq $Na_2S_2O_7$ followed by satd Na_2CO_3. The organic layer was concd in vacuo and chromatographed on SiO_2 (hexanes: EtOAc, 9:1) to give 84.4 mg (74%) of **15** as a white solid: mp 89.3–89.9 °C (hexanes:EtOAc); IR (neat) 3025, 1717, 1610, 1561, 1485, 1436, 1348, 1323, 1302, 1285, 1235, 1188, 1103, 1072, 1057, 1022 cm^{-1}; ^1H NMR 8.1–7.95 (m, 2H), 7.5–7.3 (m, 3H), 3.92 (s, 3H), 2.68 (s, 3H); ^{13}C NMR: δ 162.7, 159.5, 156.3, 130.8, 128.8, 128.6, 128.3, 126.4, 51.9, 11.98; MS (EI) *m/z* (relative intensity) 231 (6), 217 (51), 185 (55), 105 (100), 77 (41), 44 (64); HRMS (EI) *m/z* calcd for $C_{12}H_{11}NO_3$: 217.0739, found: 217.0729.

5-Methyl-2-phenyl-oxazole-4-carboxylic acid (11). A solution of 2.07 g (9.5 mmol) of **15** in 20 mL of 3 M NaOH and 12 mL of MeOH was stirred at 22 °C for 2 h and extracted with Et_2O. The aq layer was acidified to pH 1 with concd HCl and extracted with EtOAc. The organic layer was dried (Na_2SO_4), and concd in vacuo to give 1.84 g (95%) of **11** as an off-white solid: mp 182.3–182.6 °C (EtOAc:hexanes); IR (neat) 3200, 2950, 2932, 2890, 2363, 2336, 1694, 1682, 1611, 1563, 1483, 1450, 1337, 1255, 1192, 1117, 1053, 1020 cm^{-1}; ^1H NMR: δ 10.2–9.9 (br s, 1H), 8.2–7.9 (m, 2H), 7.6–7.4 (m, 3H), 2.75 (s, 3H); ^{13}C NMR: (CD_3OD) δ 164.6, 160.7, 157.4, 131.9, 129.8, 129.6, 127.3, 127.2, 12.1; MS (EI) *m/z* (rel. int.) 203 (53), 185 (24), 157 (13), 116 (17), 105 (100), 89 (21), 77 (33), 63 (16); HRMS calcd for $C_{11}H_9NO_3$: 203.0582, found: 203.0583.

Solid-phase chemistry

Step 1, 5→16. In a medium porosity Schlenk filter aparatus was placed 750 mg Wang resin (0.96 mmol/g, 0.72 mmol of active sites). The resin was suspended in 12 mL of dry DMF and a stream of nitrogen was forced up through the filter at a rate which allowed the solvent to gently bubble. To this reaction mixture was added 1.47 g (3.6 mmol) of **5**. The suspension was agitated for 5 min and treated with 26 mg (0.216 mmol) of DMAP and 550 mg (2.88 mmol) of EDCI, agitated at 22 °C for 18 h and filtered, and the resin was washed with DMF (2 × 10 mL), H_2O (3 × 10 mL), THF (3 × 10 mL), and CH_2Cl_2 (3 × 10 mL). The resin was dried under vacuum and the remaining active sites were capped by addition of 10 mL of CH_2Cl_2 and 10 mL of acetic anhydride along with 26 mg (2.88 mmol) of DMAP to the resin. Bubbling was continued at 22 °C for 3 h and the resin was then washed with CH_2Cl_2 (6 × 15 mL) and dried in vacuo. To test the loading on the resin, 30 mg of resin was removed and suspended in 2 mL of trifluoroacetic acid for 5 min at 22 °C, filtered and washed (3 × 3 mL) with CH_2Cl_2. The filtrate was concentrated in vacuo to give 7.3 mg (85%) of **5**.

Step 2, 16→17. A suspension of 690 mg (0.576 mmol) of 2-(9H-fluoren-9-ylmethoxycarbonylamino)-pentanedioic acid 5-allyl ester linked to Wang resin (**16**) in 15 mL of THF was treated with 6 mL (57.6 mmol) of piperidine, agitated by bubbling for 30 min, filtered and washed with CH_2Cl_2 (6 × 10 mL). The resin was dried in vacuo. A suspension of this resin in 10 mL of CH_2Cl_2 was treated with 0.48 mL (2.31 mmol) of decanoyl chloride and 14 mg (0.115 mmol) of DMAP. The reaction mixture was agitated at 22 °C for 6 h, filtered and the resin was washed with CH_2Cl_2 (6 × 10 mL) and dried in vacuo.

Step 3, 17→18. A suspension of 690 mg (0.576 mmol) of 2-decanoylamino-pentanedioic acid 5-allyl ester linked to Wang resin (**17**) in 10 mL of THF was treated with 67 mg (0.0576 mmol) of tetrakis(triphenylphosphine)palladium(0) and 806 mg (5.75 mmol) of dimedone, and agitated by bubbling at 22 °C for 18 h. The resin was then filtered, washed with THF (2 × 10 mL), CH_2Cl_2 (2 × 10 mL), MeOH (2 × 10 mL), H_2O (2 × 10 mL), 1% HOAc soln (2 × x10 mL), H_2O (2 × 10 mL), MeOH (2 × 10 mL), CH_2Cl_2 (2 × 10 mL), and dried in vacuo. Cleavage and examination of 40 mg of resin by ^1H NMR showed full deprotection of the allyl ester.

A suspension of this resin in 12 mL of DMF was treated with 0.22 mL (1.572 mmol) of triethylamine and 414.1 mg (2.62 mmol) of Alloc-$NHCH_2CH_2NHMe$. After agitating the reaction mixture for 5 min to ensure proper mixing, 540 mg (1.572 mmol) of CloP was added. The reaction mixture was agitated with bubbling for 18 h at 30 °C, cooled to 22 °C, and the resin was filtered and washed with DMF (2 × 10 mL), CH_2Cl_2 (2 × 10 mL), MeOH (2 × 10 mL), H_2O (2 × 10 mL), THF (2 × 10 mL), and CH_2Cl_2 (2 × 10 mL). The resin was dried in vacuo and 40 mg of resin was cleaved with CF_3CO_2H. The ^1H NMR of the residue showed that coupling had occurred to nearly 100%.

Step 5, 18→19. A suspension of 200 mg (0.192 mmol) of 4-[(2-allyloxycarbonylamino-ethyl)-methyl-carbamoyl]-2-decanoylamino-butyric acid linked to Wang resin (**18**) in 6 mL of CH_2Cl_2 was treated with 12 mg (0.0096 mmol) of tetrakistriphenylphosphine Pd(0), 62 ml (0.230 mmol) of tributyltin hydride, and 10 µl of H_2O. The reaction mixture was agitated with bubbling N_2 for 15 min, filtered, and the resin was washed with 10 mL portions of CH_2Cl_2, THF, acetone, MeOH, H_2O, acetone, EtOAc, hexanes, THF, and CH_2Cl_2. The resin was then dried in vacuo and 15 mg was removed for testing. The ^1H NMR of the TFA-cleaved residue showed full deprotection as well as full removal of all tin side products.

A suspension of 185 mg (0.190 mmol) of this resin in 8 mL of CH_2Cl_2 was treated with 117 mg (0.576 mmol) of oxazole carboxylic acid, 198 mg (0.576 mg) of CloP, and 80 µl (0.576 mmol) of triethylamine. The reaction mixture was agitated by bubbling with N_2 for 3 h, filtered, and washed with 20 mL of CH_2Cl_2, acetone, water, acetone, and CH_2Cl_2. The resin was dried in vacuo and 15 mg was removed for testing. The ^1H NMR of the residue showed that the reaction had gone to 60% completion. The resin was subsequently submitted to a second coupling cycle.

Step 6, 19→1. A suspension of 115 mg (0.12 mmol) of 2-decanoylamino-4-(methyl-{3-[5-methyl-2-phenyl-oxazole-4-carbonyl]-ethyl}-carbamoyl)-butyric acid linked to Wang resin (**19**) in 3 mL of TFA was stirred for 5 min, filtered, and washed with 5 mL of CH_2Cl_2. The extract was concd in vacuo to provide 33.1 mg (100% for step 2 to step 6) of **1**. A ^1H NMR showed the product to be 66% pure with 2-acylamino-pentanedioic acid as the major impurity. Acid **1a** was dissolved in 3 mL of CH_2Cl_2 and treated with 0.016 mL (0.138 mmol) of benzyl bromide and 0.02 mL (0.138 mmol) of DBU to provide material identical with the benzyl ester **2** prepared by solution phase chemistry.

Cell culture

Human MDA-MB-231 breast carcinoma cells were obtained from the American Type Culture Collection at passage 28 and were maintained for no longer than 20 passages. The cells were grown in RPMI-1640 supplemented with 1% penicillin (100 µg/mL) and streptomycin (100 µg/mL), 1% L-glutamate, and 10% fetal bovine serum in a humidified incubator at 37 °C under 5% CO_2 in air. Cells were routinely found free of mycoplasma. To remove cells from the monolayer for passage or flow cytometry, we washed them two times with phosphate buffer and briefly (< 3 min) treated the cells with 0.05% trypsin/2 mM EDTA at room temperature. After the addition of at least two volumes of growth medium containing 10% fetal bovine serum, the cells were centrifuged at 1000*g* for 5 min. Compounds were made into stock solns using DMSO, and stored at −20 °C. All compounds and controls were added to obtain a final concn of 0.1–0.2% (v/v) of the final soln for experiments.

PP2A assay

The activity of the catalytic subunit of bovine cardiac muscle PP2A (Gibco-BRL, Gaithersburg, MD) was measured with fluorescein diphosphate (Molecular Probes, Inc., Eugene, OR) as a substrate in 96-well microtiter plates. The final incubation mixture (150 µL) comprised 25 mM Tris (pH 7.5), 5 mM EDTA, 33 µg/mL BSA, and 20 µM fluorescein diphosphate. Inhibitors were resuspended in DMSO, which was also used as the vehicle control. Reactions were initiated by adding 0.2 units of PP2A and incubated at room temperature overnight. Fluorescence emission from the product was measure with Perseptive Biosystems Cytoflour II (exciton filter, 485 nm; emission filter, 530 nm) (Framingham, MA).

Cell proliferation assay

The antiproliferative activity of newly synthesized compounds was determined by our previously described method.[46] Briefly, cells (6.5×10^3 cells/cm^2) were plated in 96 well flat bottom plates for the cytotoxicity studies and incubated at 37 °C for 48 h. The plating medium was aspirated off 96 well plates and 200 µL of growth medium containing drug was added per well. Plates were incubated for 72 h, and then washed 4× with serum free medium. After washing, 50 µL of 3-[4,5-dimethylthiazol-2-yl]-2,5-diphenyl tetrazolium bromide soln (2 mg/mL) was added to each well, followed by 150 µL of complete growth medium. Plates were then incubated an additional 4 h at 37 °C. The soln was aspirated off, 200 µL of DMSO added, and the plates were shaken for 30 min at room

temperature. Absorbance at 540 nm was determined with a Titertek Multiskan Plus plate reader. Biologically active compounds were tested at least three independent times.

Measurement of cell cycle kinetics

Cells (6.5×10^5/cm^2) were plated and incubated at 37 °C for 48 h. The plating medium was then aspirated off, and medium containing a concentration of compound **1f** that caused approximately 50% growth inhibition (88–100 μM) was added for 48–72 h. Untreated cells at a similar cell density were used as control populations. Single cell preparations were fixed in ice-cold 1% paraformaldehyde, centrifugation at 1000 *g* for 5 min, resuspended in Puck's saline, centrifuged, and resuspended in ice-cold 70% ethanol overnight. The cells were removed from fixatives by centrifugation (1000 *g* for 5 min) and stained with a 5 μg/mL propidium iodide and 50 μg/mL RNase A solution. Flow cytometry analyses were conducted with a Becton Dickinson FACS Star. Single parameter DNA histograms were collected for 10,000 cells, and cell cycle kinetic parameters calculated using DNA cell cycle analysis software version C (Becton Dickinson). Experiments at 72 h were performed at least three independent times.

Acknowledgment

Funding was provided by the American Cancer Society (Junior Faculty Research Award to P.W.), Upjohn Co., the Alfred P. Sloan Foundation. and a United States Army Breast Cancer Predoctoral Fellowship. We thank Drs Boynton and Messner for their preliminary biochemical evaluation of **1a-r**.

References and Notes

1. Johnson, L. N.; Barford, D. *Annu. Rev. Biophys. Biomol. Struct.* **1993**, *22*, 199.

2. (a) Murray, K. J.; Warrington, B. H. In *Comprehensive Medicinal Chemistry;* (Sammes, P. G.; Taylor, J. B., Eds.; Pergamon Press: Oxford, 1990; Vol. 2; Chapter 8.7; p 531. (b) Murray, K. J.; Coates, W. J. *Annu. Rep. Med. Chem.* **1994**, *29*, 255.

3. Zolnierowicz, S.; Hemmings, B. A. *Trends in Cell Biol.* **1994**, *4*, 61.

4. Honkanen, R. E.; Boynton, A. L. In *Protein kinase C*; J. F. Kuo, Ed.; Oxford University Press: Oxford, 1994; Chapter, 12; p 305, and references cited therein.

5. Song, Q.; Baxter, G. D.; Kovacs, E. M.; Findik, D.; Lavin, M. F. *J. Cell. Phys.* **1992**, *153*, 550.

6. Haldari, S.; Jena, N.; Croce, C. M. *Proc. Natl Acad. Sci. U.S.A.* **1995**, *92*, 4507.

7. Boe, R.; Gjertsen, B. T.; Vintermyr, O. K.; Houge, G.; Lanotte, M.; Doskeland, S. O. *Exp. Cell. Res.* **1991**, *195*, 237.

8. Kiguchi, K.; Glesne, D.; Chubb, C. H.; Fujiki, H.; Huberman, E. *Cell Growth Differentiation* **1994**, *5*, 995.

9. Xia, Z.; Dickens, M.; Raingeaud, J.; Davis, R. J.; Greenberg, M. E. *Science* **1995**, *270*, 1326.

10. Mumby, M. C.; Walter, G. *Physiol. Rev.* **1993**, *73*, 673.

11. Wera, S.; Hemmings, B. A. *Biochem. J.* **1995**, *311*, 17.

12. Fujiki, H.; Suganuma, M.; Yatsunami, J.; Komori, A.; Okabe, S.; Nishiwakimatsushima, R.; Ohta, T. *Gazz. Chim. Ital.* **1993**, *123*, 309.

13. Nishiwaki, S.; Fujiki, H.; Suganuma, M.; Furuya-Suguri, H. *Carcinogenesis* **1990**, *11*, 1837.

14. (a) Takai, A.; Murata, M.; Torigoe, K.; Isobe, M.; Mieskes, G.; Yasumoto, T. *Biochem. J.* **1992**, *284*, 539. (b) Sasaki, K.; Murata, M.; Yasumoto, T.; Mieskes, G.; Takai, A. *Biochem. J.* **1994**, *288*, 259.

15. Rinehart, K. L.; Namikoshi, M.; Choi, B. W. *J. Appl. Phycol.* **1994**, *6*, 159.

16. De Silva, E. D.; Williams, D. E.; Andersen, R. J.; Klix, H.; Holmes, C. F. B.; Allen, T. M. *Tetrahedron Lett.* **1992**, *33*, 1561.

17. Bagu, J. R.; Sonnichsen, F. D.; Williams, D.; Andersen, R. J.; Sykes, B. D.; Holmes, C. F. *Nature Struct. Biol.* **1995**, *1*, 114.

18. Valentekovich, R. J.; Schreiber, S. L. *J. Am. Chem. Soc.* **1995**, *117*, 9069.

19. Matsuzawa, S.; Suzuki, T.; Suzuki, M.; Matsuda, A.; Kawamura, T.; Mizuno, Y.; Kikuchi, K. *FEBS Lett.* **1994**, *356*, 272.

20. Li, Y.-M.; Casida, J. E. *Proc. Natl Acad. Sci. U.S.A.* **1992**, *89*, 11867.

21. Eldridge, R.; Casida, J. E. *Tox. Appl. Pharm.* **1995**, *130*, 95.

22. Li, V. M.; Mackintosh, C.; Casida, J. E. *Biochem. Pharm.* **1993**, *46*, 1435.

23. (a) Evans, D. A.; Gage, J. R.; Leighton, J. L. *J. Am. Chem. Soc.* **1992**, *114*, 9434. (b) Ichikawa, Y.; Tsuboi, K.; Jiang, Y.; Naganawa, A.; Isobe, M. *Tetrahedron Lett.* **1995**, *36*, 7101.

24. Very recently, it was reported that tautomycin acts in its hydrolysed, bis-carboxylic acid form: Sugiyama, Y.; Ohtani, I. I.; Isobe, M.; Takai, A.; Ubukata, M.; Isono, K. *Bioorg. Med. Chem. Lett.* **1996**, *6*, 3.

25. Honkanen, R. E.; Codispoti, B.; Tse, K.; Boynton, A. L. *Toxicon* **1994**, *32*, 339.

26. Takai, A.; Sasaki, K.; Nagai, H.; Mieskes, G.; Isobe, M.; Isono, K.; Yasumoto, T. *Biochem. J.* **1995**, *306*, 657.

27. Yoshizawa, S.; Matsushima, R.; Watanabe, M. F.; Harada, K.; Ichihara, A.; Carmichael, W. W. *Cancer Res. Clin. Oncol.* **1990**, *116*, 609.

28. MacKintosh, C.; Klumpp, S. *FEBS Lett.* **1990**, *277*, 137.

29. Honkanen, R. E.; Zwiller, J.; Moore, R. E.; Daily, S. L.; Khatra, B. S.; Dukelow, M.; Boynton, A. L. *J. Biol. Chem.* **1990**, *265*, 19401.

30. (a) Quinn, R. J.; Taylor, C.; Suganuma, M.; Fujiki, H. *Bioorg. Med. Chem. Lett.* **1993**, *3*, 1029. (b) Taylor, C.; Quinn, R. J.; McCulloch, R.; Nishiwaki-Matsushima, R.; Fujiki, H. *Bioorg. Med. Chem. Lett.* **1992**, *2*, 299.

31. (a) Gallop, M. A.; Barrett, R. W.; Dower, W. J.; Fodor, S. P. A.; Gordon, E. M. *J. Med. Chem.* **1994**, *37*, 1233. (b) Gordon, E. M.; Barrett, R. W.; Dower, W. J.; Fodor, S. A.; Gallop, M. A. *J. Med. Chem.* **1994**, *37*, 1385.

32. Wipf, P.; Cunningham, A. *Tetrahedron Lett.* **1995**, *36*, 7819.

33. Wipf, P. *Chem. Rev.* **1995**, *95*, 2115, and references cited therein.

34. Belshaw, P.J.; Mzengeza, S.; Lajoie, G. *Syn. Commun.* **1990**, *20*, 3157.

35. Dangles, O.; Guibe, F.; Balavoine, G.; Lavielle, S.; Marquet, A. *J. Org. Chem.* **1987**, *52*, 4984.

36. Castro, B.; Dormoy, J.-R.; Evin, G.; Selve, C.; *Tetrahedron Lett.* **1975**, *14*, 1219.

37. Wipf, P.; Miller, C. P. *J. Org. Chem.* **1993**, *58*, 3604.

38. Wang, S.-S. *J. Am. Chem. Soc.* **1973**, *95*, 1328.

39. Coste, J.; Frerot, E.; Jouin, P. *J. Org. Chem.* **1994**, *59*, 2437.

40. Dormoy, J.; Castro, B. *Tetrahedron Lett.* **1979**, *35*, 3321.

41. Department of Molecular Medicine, Northwest Hospital, Seattle, WA.

42. Hunter, T.; Pines, J. *Cell* **1994**, *79*, 573.

43. Rice, R. L.; Wipf, P.; Cunningham, A.; Lazo, J. S. *Proc. Am. Assoc. Cancer Res.* **1996**, *37*, 2896.

44. Ishida, Y.; Furukawa, Y.; Decaprio, J. A.; Saito, M.; Griffin, J. D. *J. Cell. Physiol.* **1992**, *150*, 484.

45. Jinno, S.; Suto, K.; Nagata, A.; Igarashi, M.; Kanaoka, Y.; Nojima, H.; Okayama, H. *EMBO J.* **1994**, *13*, 1549.

46. Lazo, J. S.; Kondo, Y.; Dellapiazza, D.; Michalska, A. E.; Choo, K. H.; Pitt, B.R. *J. Biol. Chem.* **1995**, *270*, 5506.

(*Received in U.S.A.* 2 *February* 1996; *accepted* 31 *May* 1996)